



Evaluation of the Use of UAV Photogrammetry for Rock Discontinuity Roughness Characterization

Riccardo Salvini¹ · Claudio Vanneschi² · John S. Coggan³ · Giovanni Mastrocrocco⁴

Received: 29 May 2019 / Accepted: 10 April 2020 / Published online: 28 April 2020
© Springer-Verlag GmbH Austria, part of Springer Nature 2020

Abstract

This paper describes the results of a field investigation with the objective of evaluating the possibility to produce drone-derived 3D digital point clouds sufficiently dense and accurate to determine discontinuity surface roughness characteristics. A discontinuous rock mass in Italy was chosen as the investigation site and Structure from Motion and Multi-View Stereo techniques adopted for producing three-dimensional point clouds from the two-dimensional image sequences. Since the roughness of discontinuities depends on direction, scale and resolution of the sampling, data were always collected along the maximum slope gradient. The scale effect was evaluated by analysing discontinuity profiles of different lengths (10 cm, 30 cm, 60 cm and 100 cm), with measurements taken from drone flights flown at different distances from the rocky slopes (10 m, 20 m and 30 m). The accuracy of the derived joint roughness coefficients was evaluated by direct comparison with discontinuity profiles measured during fieldwork using conventional techniques and from contemporaneous terrestrial laser scanning. Results from this research show that 3D digital point clouds, derived from the processing of drone-flight images, were successfully used for reliable representation of discontinuity roughness for profiles longer than 60 cm, whereas less reliable results were achieved for shorter profile lengths. This, even if strictly related to this case study since several factors can affect the minimum profile length, represents a significant contribution to improve the knowledge on the use of remotely captured data for characterising the discontinuities in natural or man-made rock outcrops, particularly where access difficulties do not allow conventional engineering-geological surveys to be undertaken.

Keywords Roughness · Rock discontinuities · Unmanned aerial vehicle · Engineering-geological survey · Terrestrial laser scanning

1 Introduction

The engineering response of natural rock masses, in particular those within a few hundred metres from the surface, are generally influenced by discontinuities (ISRM 1978),

and require a detailed knowledge of the geometrical and mechanical properties of the discontinuity network. Discontinuity characteristics, including surface roughness, can be carefully described and used to understand the overall rock mass quality and the mechanical behaviour of rock masses. It is well established that in the case of clean rough defects, the roughness (considering such properties as the amplitude and the shape of the asperities) controls the shear strength of critical discontinuities together with their mechanical properties, the shear direction and the applied normal stress (Patton 1966; Barton 1973).

Various methods have been developed to measure and characterize discontinuity roughness: the morphology of discontinuities can be measured using manual and subjective methods that require physical contact with the surface to be measured (Barton 1973, 1982; Barton and Choubey 1977; Maerz et al. 1990; Myers 1962) and highly sophisticated remote and automatic optical methods (Feng et al.

✉ Riccardo Salvini
riccardo.salvini@unisi.it

¹ Department of Environment, Earth and Physical Sciences and Centre for GeoTechnologies CGT, University of Siena, Via Vetri Vecchi 34, 52027 San Giovanni Valdarno, AR, Italy

² CGT SpinOff s.r.l., Via Vetri Vecchi 34, 52027 San Giovanni Valdarno, AR, Italy

³ Camborne School of Mines, University of Exeter, Penryn, Cornwall, UK

⁴ Apex Surveys, Unit 78, Dunboyne Business Park, Dunboyne, Co. Meath, Ireland

2003; Rahman et al. 2006; Baker et al. 2008; Sturzenegger and Stead 2009; Tatone and Grasselli 2009; Ge et al. 2015). The former approaches require field observations, using for example Barton's profilometer or roughness gauge and corresponding joint roughness coefficient values (JRC—Barton and Choubey 1977). Direct field observations can, however, expose personnel to potentially hazardous and dangerous situations due to the need for physical access to the exposed rock outcrops. Alternatively, the latter approaches use advanced technologies to remotely acquire morphological information, generally represented by images and 3D point clouds that can complement and, in certain instances, supplement traditional engineering-geological surveys for characterization of the rock outcrops. These techniques allow data collection from a certain distance from the rock face in accordance with the instrument specifications and the required data resolution or outcome detail, reducing acquisition time and improving worker's safety.

Methods, such as terrestrial laser scanning (TLS) and digital photogrammetry (DP), have become well-established techniques in rock mass characterization (Sturzenegger and Stead 2009; Firpo et al. 2011; Salvini et al. 2011, 2017; Assali et al. 2014; Deliormanli et al. 2014; Vanneschi et al. 2014, 2017; Francioni et al. 2014, 2015; Riquelme et al. 2017; Mastrococco et al. 2018). TLS allows for rapid acquisition of detailed information of rock surfaces with generation of high resolution point clouds (with a millimetre level of detail) that has been shown in the literature to be an accurate and efficient approach for quantification of rock surface roughness, despite the potential negative influence of data noise (Heritage and Milan 2009; Khoshelham et al. 2011; Mills and Fotopoulos 2013; Bitenc et al. 2015; Ge et al. 2015). Recently, Fan and Cao (2019) conducted a series of direct shear tests on rock joints at a lab-scale with random surface morphology under various constant normal loads. Joint surface morphologies of 15 specimens at laboratory scales were scanned by high precision laser scanning and the joint surface morphologies digitized into point data. From the investigation, they concluded that the arithmetic conversion of 3D joint surface morphology into a 2D average height joint profile is reliable for study of joint shear mechanical characteristics.

Digital photogrammetry (DP) is also widely recognized as a valid approach for geometric rock mass characterization. Several studies have been undertaken for quantification of rock surface roughness (Haneberg 2008; Nilsson and Wulkan 2011; Bretar et al. 2013; Kim et al. 2013b; Sirkiä et al. 2016; Corradetti et al. 2017; Unal et al. 2017). The determination of joint roughness is, however, scale-dependent (Barton 1973) and the level of detail obtained from DP models is related to data acquisition techniques employed and image algorithms used to post-process the images and/or scenes. Importantly, only in the last few years has reproduction of

3D models of rock masses become possible with a sub-centimetre level of detail, due to recent improvements of DP; in particular, the availability of high-performance digital cameras (both in geometry and radiometry) and powerful image processing algorithms for the reconstruction of 3D models.

This continuous technological enhancement is complemented by correct application and understanding of photogrammetric knowledge. This includes, correct use of interior camera calibration parameters, acquisition of well-defined images and associated network geometry, execution of accurate topographic surveys for the collection of ground control point coordinates, inclusion of check points and correct 3D point cloud production and editing.

Haneberg et al. (2006) and Haneberg (2008) confirm that directional roughness profiles and JRC can be calculated from 3D digital outcrop models derived from photogrammetry. Poropat (2008, 2009) provides a review of the use of 3D imaging for the measurement of roughness and provided some examples of measurement. He concluded that, in contrast to methods requiring physical contact with a surface, the development of precise laser scanning systems and photogrammetry systems allows estimation of surface roughness in the field without physical contact with the surface being measured.

Nevertheless, a significant problem with the use of 3D point clouds for the estimation of JRC of an exposed discontinuity is the presence in the point cloud data of errors, which may be significant enough to overestimate the JRC. The principal measurement error that must be considered is the range from the sensor to a point on an exposed discontinuity. Range errors in TLS data arise from a number of effects which may include, but are not limited to: (i) resolution limits in the range measurement, (ii) timing 'jitter' in the electronics used to measure time of flight, (iii) effect of surface reflectivity changes, and (iv) atmospheric effects. Range errors in 3D data obtained using DP may arise from several sources, including: (i) resolution limits in the disparity measurement in images, (ii) errors in the calibration of the cameras, (iii) effect of image processing algorithms, and (iv) atmospheric effects. Hence, data acquired by these systems and subsequently used for roughness estimation must take into consideration these limitations.

A further limitation of both TLS and DP in field applications, is related to the potential for occlusions and shadow-zone problems in both the horizontal and vertical direction (Sturzenegger et al. 2007). The use of a unmanned aerial vehicle (UAV) equipped either with a digital camera or laser scanning systems can, however, be utilized to minimize and overcome these vertical and horizontal issues. For example, Salvini et al. (2018) showed how, in challenging environments characterized by high steep rock faces, use of a UAV coupled with Structure from Motion (SfM; Spetsakis and Aloimonos 1991; Westoby et al. 2012; Fonstad et al. 2013;

Colomina and Molina 2014)) and Multi-View Stereo (MVS; Gallup et al. 2007; Goesele et al. 2007; Jancosek et al. 2009) techniques can be used for rock mass characterization and hazard assessment. Due to technological improvements, attempts to obtain discontinuity roughness measurements from DP processed with SfM–MVS technique have become more common. For example, Marsch and Wernecke (2015) compared JRC values obtained from traditional profilometers to DP/SfM derived profiles. They suggested that care should be used since significant differences may be detected between the two methods.

Most previous studies are related to use of terrestrial photogrammetric approach, and do not refer to UAV photogrammetry, where limitations of flight characteristics and environmental factors (dust, wind, heterogeneous light conditions, rain, fog, etcetera) must also be considered. Generally, field-derived data may have a level of accuracy lower than that estimated from tests executed in a controlled environment, such as a laboratory, or by using terrestrial photogrammetry, where there is the possibility to take higher quality images. Karekal et al. (2013) applied a 3D imaging technique developed by CSIRO™ to obtain 3D surface models of concrete blocks that replicated, in laboratory, the surface roughness of discontinuities in sandstone samples. They found that modelled surface damage and comparisons with those observed experimentally correlated reasonably well, allowing them to conclude that 3D point clouds remotely collected can be adopted also to estimate the roughness in the exposed joint surfaces of open pit mines.

Kim et al. (2016) investigated, under field conditions, the differences on 30 JRC values obtained on rock outcrops with traditional (profilometer) and geomatic (SfM point cloud) approaches. They found that under field conditions, data noise is present in the 3D point cloud and only high-resolution data (point interval ≤ 1 mm) can reduce the JRC correspondence errors. In addition, Kim et al. (2018) showed that when using close-range photogrammetry, without an adequate statistical treatment of the point cloud data, data errors may overestimate JRC values.

The JRC is the most widespread method used to estimate the discontinuity roughness and, together with other parameters, is used to establish the geotechnical behaviour of a rock mass (i.e. friction angle) and the shear strength of discontinuities. Traditionally, the JRC determination utilizes the Barton (1982) method, which is based on the use of a traditional profilometer and comparison to published JRC profile values. This is not the only method used by the scientific community to obtain JRC data. Alternative approaches, such as the tilt test (Barton and Choubey 1977) and Maerz et al. (1990) or Tse and Cruden (1979) methods, exist. Several authors (such as Grasselli et al. 2002; Grasselli and Egger 2003; Milne et al. 2009; Kim et al. 2013a) have questioned the reliability of reproducing JRC linear profiles,

mainly because of the subjectivity of the original traditional approach. Nevertheless, the determination of JRC from Barton's profilometer or comb and comparison to published values is still a widespread method, with the advantage of having an extensive collection of case histories where this technique has been successfully applied. The focus of the present paper is not to find a new method for estimating the JRC values, but only to understand if, and how, UAV-based point clouds can be used for joint roughness measurements.

Use of a UAV for this research is to avoid the need for physical access to rock surfaces. UAV flights also overcome some limitations of traditional TLS surveys such as: (i) possible bias due to the angle between the laser beam and the discontinuities, (ii) numerous scans from different locations to avoid shadows, (iii) possible unavoidable shadows or vertical biases in the case of high and inaccessible rock faces. A multicopter UAV can fly in front of every discontinuity, acquiring images from several different locations, both in the horizontal, oblique, and vertical direction.

In this investigation, a discontinuous rock mass outcrop in Italy was chosen as the study site to critically evaluate whether, at which scale and to which image resolution, a UAV/SfM–MVS approach can be used to quantify rock joint surface roughness. Images were captured at different ranges from the rock outcrop to evaluate JRCs with a different scale of detail. The point cloud-derived data were then compared with those manually and remotely measured by traditional engineering-geological and TLS surveys. Attention was given to the fact that the roughness of a discontinuity depends on direction, scale and resolution of the sampling (Ge et al. 2015). For this reason, the JRCs were investigated along the shear direction, and the scale effect evaluated by analysing profiles of different lengths (10 cm, 30 cm, 60 cm and 100 cm).

The aim of this paper is to perform a practical field investigation evaluating the reliability of discontinuity surface roughness measurements taken from UAV-derived point clouds. The key purpose of the work is to verify the possibility of obtaining JRCs with a level of accuracy comparable to those commonly accepted in direct engineering-geological surveys through use of a conventional profilometer. Such a possibility would represent an improved understanding of the use of remotely captured data for discontinuity characterization in engineering-geological investigations and provide evidence for confidence in their use for such purposes.

2 Study Area and Geological Setting

The area of study is in the southern part of the Montegrossi open pit (Siena, Italy), an inactive extraction site of aggregates mainly made of calcarenites. The quarry is located in the Chianti ridge, also called "Monti del Chianti", consisting

of a closely spaced chain of hills, NNW-SSE oriented and more than 35 km in length (Fig. 1). The Monti del Chianti ridge is a morphologic element of Neogene age (Elter and Sandrelli 1994; Fazzuoli et al. 1994; Bonini 1999), that separates intermontane late Miocene-Pliocene sedimentary basins to the west (Siena and surrounding basins) from the continental Plio-Pleistocene Upper Valdarno Basin, to the east (Pandeli et al. 2018).

The main tectonic structure of the Monti del Chianti area consists of an asymmetric to overturned/recumbent anti-form of the Tuscan Nappe, whose axis is oriented NNW-SSE (Valduga 1948, 1952; Merla 1951). The main structural features of the Tuscan Nappe in Monti del Chianti Ridge are well exposed at the mesoscale in the Montegrossi quarry. Here, the main structure is defined by hectometre-kilometre scale NE-vergent overturned to recumbent folds, closely associated with parasitic folds (metre to decametre scale) characterized by a NW-SE and NNW-SSE axial strike (Fazzuoli et al. 2004). These folds are in turn deformed by a successive family of folds, showing sub-vertical to SW steeply dipping axial planes. Subsequent high-angle normal faults systems, with trends mainly oriented NW-SE, WNW-ESE, NE-SW and NS, dissected the orogenic pile of nappes; among them, the NW-SE trending high-angle fault system may be considered the main system of the study

area and is characterized by dips of about 70° to SW and, subordinately, to NE.

In the study area, lithotypes belonging to the Scaglia Toscana Formation and the overlying Macigno Formation (Bortolotti et al. 1970; Fazzuoli et al. 1994), two of the most widely outcropping lithostratigraphic units of the Northern Apennines, outcrop (Fig. 2).

According to the subdivision of the Cretaceous to Oligocene Scaglia Toscana Formation in the Monti del Chianti proposed by (Fazzuoli et al. 1996, 2004), the following members were identified in the study area: Marne del Sugame, Calcareni di Montegrossi and Argilliti e Calcareni di Dudda (Fig. 2). In this context, the slope under study is completely made of calcarenites of the Montegrossi Member (STO3 in Fig. 2) and it has dip direction/dip values of 320/65, respectively, with a mean elevation of 570 metres above sea level (m.a.s.l.). This member consists of calcarenites and calcirudites, often cherty, alternating with thin beds of shales and marls. The thickness is up to 120 m, with a maximum value of about 200 m (Nocchi 1960). The lower part of the member is traditionally attributed to the late Cretaceous whereas the middle and the upper part to the Paleocene-Eocene through foraminifers (Nocchi 1960; Canuti et al. 1966).

The rock mass is characterized by stratigraphic beds (named B in Fig. 3), typically tabular at the outcrop scale with lenticular beds locally occurring, whose thickness generally varies from 30 cm to 3 m with a dip direction/dip respectively of 85/60°. Also, two main sets of discontinuities are present with nominal attitude values of 350/80 (K1 in Fig. 3) and 270/50 (K2 in Fig. 3), respectively.

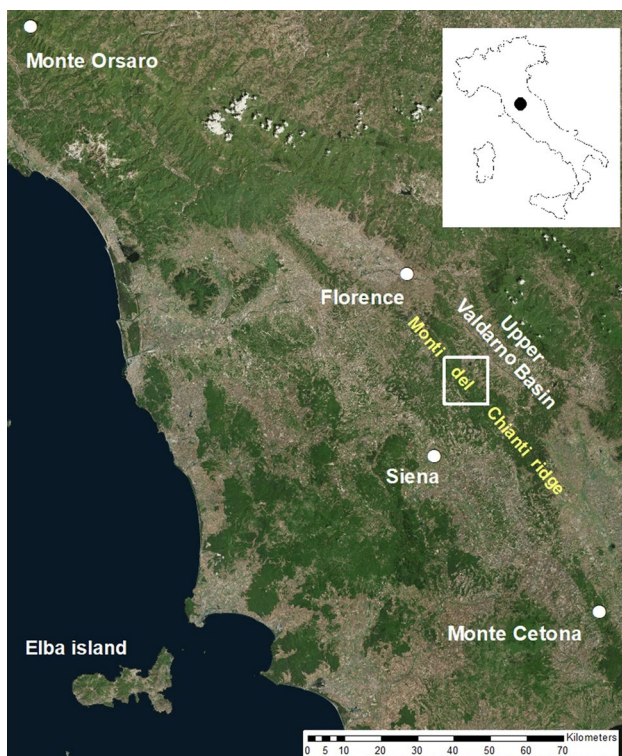


Fig. 1 Satellite view of the study area represented by the white rectangle. Inset map shows the location in Italy

3 Methods

3.1 Engineering-Geological Investigation

To directly measure roughness profiles of calcarenites beds and joints, and to characterise the main geomechanical properties of discontinuities, a traditional engineering-geological survey of the site was carried out. Data were collected in the same outcrops to that investigated by UAV and TLS, and the same strata were measured. A number of discontinuities characteristics were collected, including the following: dip direction/dip (degree), spacing (m), length (m), persistence (%), termination (typology), aperture (mm), infilling (type), infilling width (mm), weathering (type), JRC, number (n) of rebounds from the Schmidt hammer measured both of the unaltered rock and the discontinuity surfaces and groundwater conditions. Discontinuity roughness was measured by using two different profilometers, 10 cm and 30 cm long, and the JRC was determined by using the Barton (1982) method,

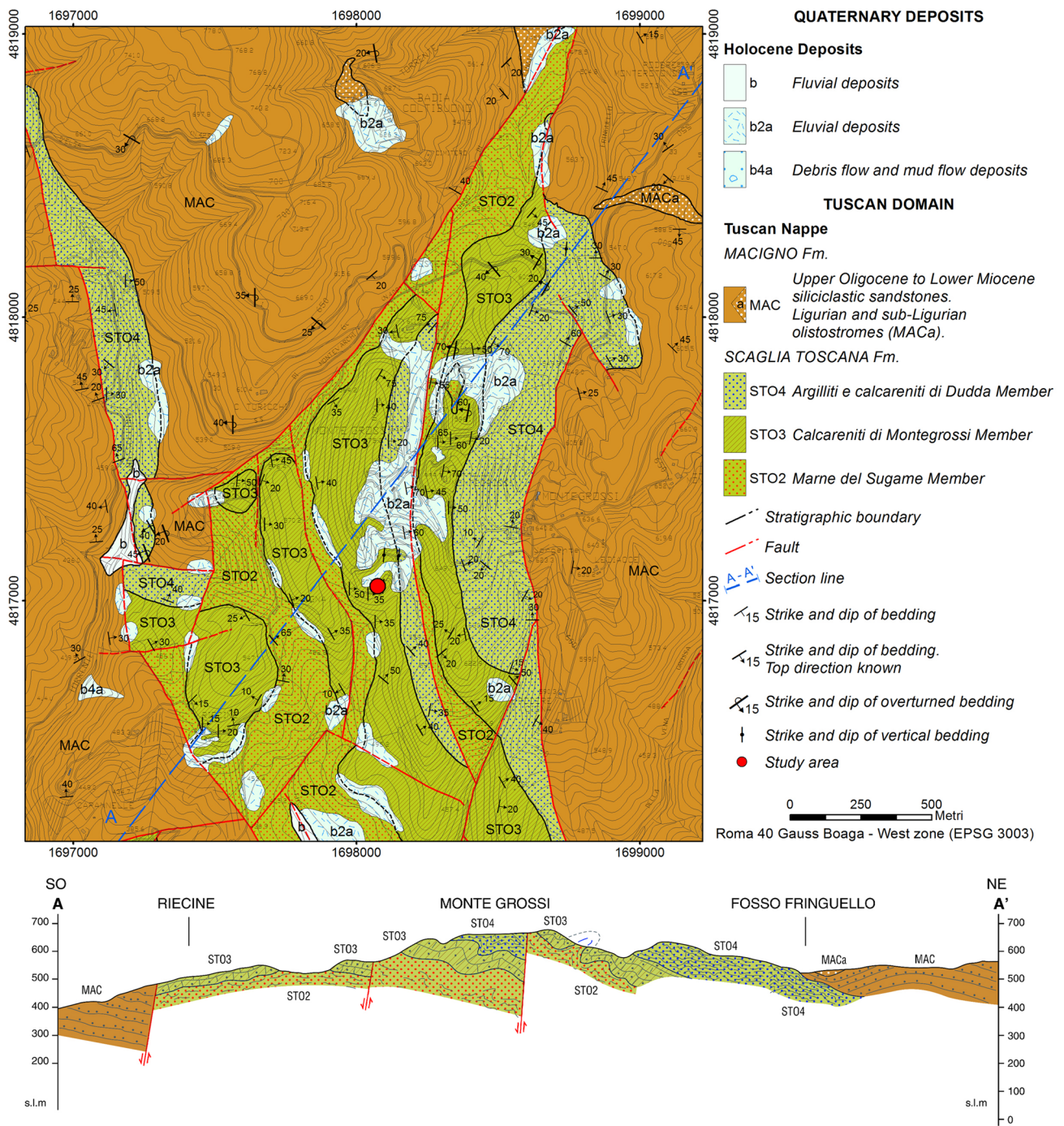


Fig. 2 Geological map of the Montegrossi area modified from the national geological cartographic “CARG” project of the Geological Survey of Italy (ISPRA) and Tuscany Region

which allows for JRC estimation of profiles with different lengths (Fig. 4).

From literature and practice, it is known that the accuracy of JRC can be strongly affected by personal bias. Since accurate determination of JRC is essential for evaluating the possibility of using UAV photogrammetry for joint surface roughness estimation, every measurement in the field was

complemented by a photograph of the profile (captured with the aim of being able to check, in laboratory, the correctness of the assigned JRC value). Images were also used for drawing vector profiles to be compared with the ones derived, on the same discontinuities, from the UAV and TLS point clouds.

3.2 UAV Survey and Image Processing

Three UAV surveys were carried out during fieldwork with a photo acquisition direction quasi-perpendicular to the rock faces. The surveys were performed using an Aibotix™ Aibot X6 V1 multicopter, which has six electric rotors, equipped with a Nikon™ CoolpixA digital camera (Table 1) and a Global Navigation Satellite System/Inertial Measurement Unit (GNSS/IMU) system. This allowed recording of 3D coordinates (X_0, Y_0, Z_0) and orientation of the camera (pitch, roll, yaw— ω, ϕ, κ) at every shoot or image.

Figure 5 shows the photogrammetric network design of the surveys that were manually performed through single quasi-parallel flight lines at three different distances from the quarry slope: 10 m, 20 m and 30 m, respectively. For every single flight a total of 98, 51 and 40 images, respectively, were acquired with a nominal overlap and sidelap greater than 80% and 60%.

The average estimated distances between pixel centres measured on the ground (i.e. Ground Sample Distance—GSD) were equal to 2.5, 5.5 and 7.5 mm for the three flights 10 m, 20 m and 30 m distant from the slope, respectively.

GSDs were chosen in consideration of the millimetric detail necessary whereby roughness profiles were reconstructed. For determining the detail of the spatial data acquired there is a geometric inter-relationship between focal length, pixel size, baseline length and distance from

the object being measured. The accuracy of the photogrammetric process depends on the correctness of image acquisition but also on the availability of a full topographic survey. During the flights, a reflectorless Total Station (TS) survey was also carried out to ensure georeferencing and the necessary spatial accuracy of the resultant model. A series of artificial targets (11 targets in total), 20×20 cm, were placed on the slope with the purpose of obtaining an optimum spatial distribution on the accessible zones of the study area (Fig. 6). Two GNSS receivers, operating in static modality for a time span longer than three hours, were used to obtain the geographic coordinates of two points: the origin of the TS survey and its zero-Azimuth direction. GNSS data were corrected using contemporary data recorded by permanent GNSS stations of the Leica Smartnet Italpos network (i.e. Siena, Rassina and Calenzano) thereby allowing millimetric accuracy. Ellipsoidal heights were converted to orthometric heights by using Convergo, an Italian code for full coordinate conversion. By using the absolute coordinates of the two GNSS points, a 3D roto-translation of all the targets was performed and their coordinates were assigned to the UTM-ETRF2000 Zone 32 N coordinate system.

Images acquired during the UAV flights were processed within Agisoft™ Photoscan Professional 1.2.5 (Agisoft 2016). This software resolves equations for interior and exterior orientation of images and can generate georeferenced spatial data, such as 3D point clouds, digital surface

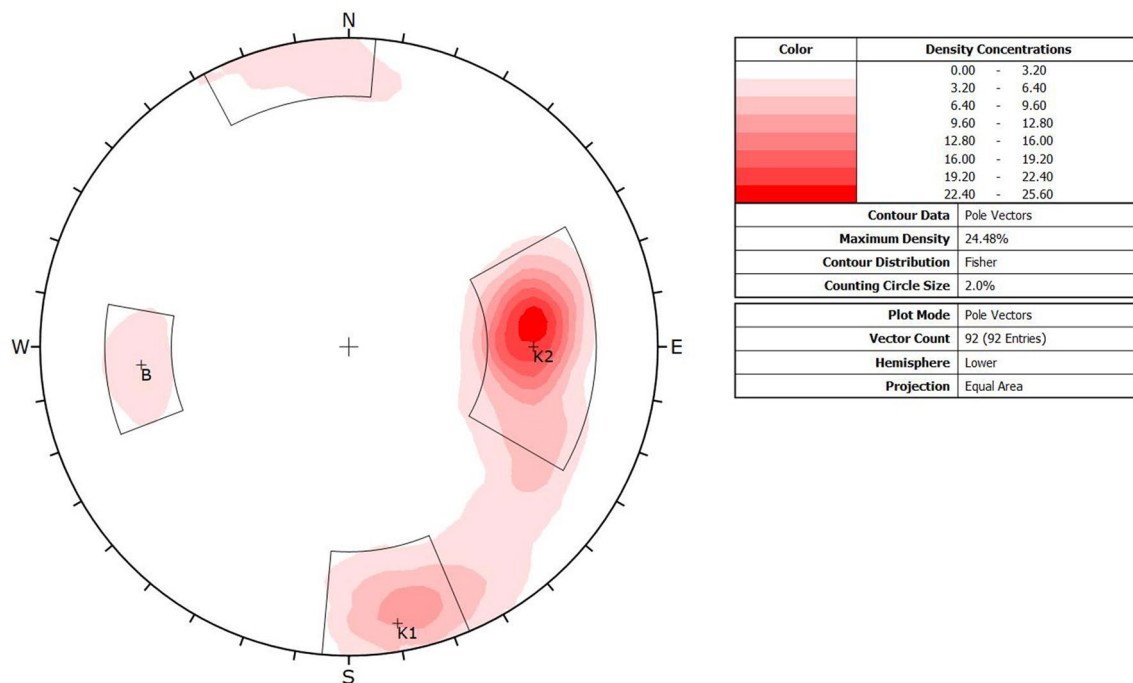


Fig. 3 Stereonet plot of discontinuity poles (Schmidt, equal area, lower hemisphere) manually collected during traditional engineering-geological survey

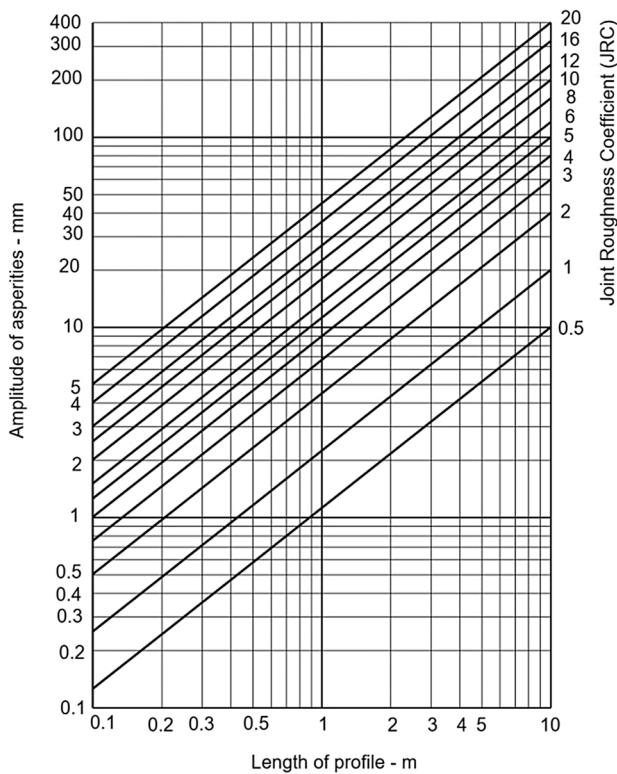


Fig. 4 Chart showing Barton (1982) method for JRC estimation from measurements of surface roughness amplitude in profiles of different length

models (DSMs) and orthophotos. Images were processed with an identical photogrammetric method for the three distinct Agisoft™ Photoscan projects for the flights at different distances from the slope. The first processing step consisted of images alignment, through which the interior and relative orientation parameters of scenes were solved. To improve the whole alignment process and to obtain low re-projection errors, millions of tie points were automatically extracted without setting a point limit.

Following image alignment, the second processing step involved georeferencing of the 3D model to solve the exterior orientation parameters by using Ground Control Points (GCPs) coordinates measured during the GNSS-TS topographic survey. The exterior orientation of images was necessary to measure dips and dip directions of slopes and discontinuities. All the artificial targets, 11 in total, were identified directly on the images. Subsequently, the ‘optimize’ tool was utilized to adjust the estimated camera positions and to remove possible non-linear deformations, minimizing the errors due to re-projection and misalignment of the photos. In addition, the optimization was improved by deleting all the tie points with a re-projection error greater than 1 pixel. In a final step, 3D dense point clouds were generated with “Ultra High quality” and “Mild Depth Filtering mode” settings. The “Depth Filtering” mode is typically used for identifying and removing erroneous points, known as outliers. For this study, due to the need of analyzing small details on the discontinuities (i.e. amplitude of asperities), the “Mild Depth Filtering” option was chosen since it provided the best results in terms of accuracy of the roughness profiles without losing important features that could have been erroneously considered as outliers. Differently, no point cloud sampling procedures were adopted, since this would have possibly affected the profiles accuracy. Moreover, such operation would have required a study of the appropriate sample rate that would permit to capture all the necessary details of the point cloud without any loss of information; this deepening of the research was considered beyond the scopes of this work. Finally, no automatic classification of point clouds was necessary since no vegetation or buildings were present within the area of interest.

3.3 Terrestrial Laser Scanning

An additional comparison of the joint roughness profiles was done by using 3D data from a georeferenced TLS survey

Table 1 Utilized UAV and camera specifications

UAV type	Dimensions (cm)	Engines	Rotor diameter (cm)	Empty weight (kg)	Max. take-off weight (kg)
Aibotix Aibot X6 v1	Width 105 Height 45	Brushless motors	30.48 (12")	2.45	6.5
Camera	Sensor type	Sensor Size (mm)	Image size (pixel)	Pixel size (mm)	Focal length (mm)
Nikon Coolpix A	CMOS	23.6×15.6	4928×3264	0.0047	18.5



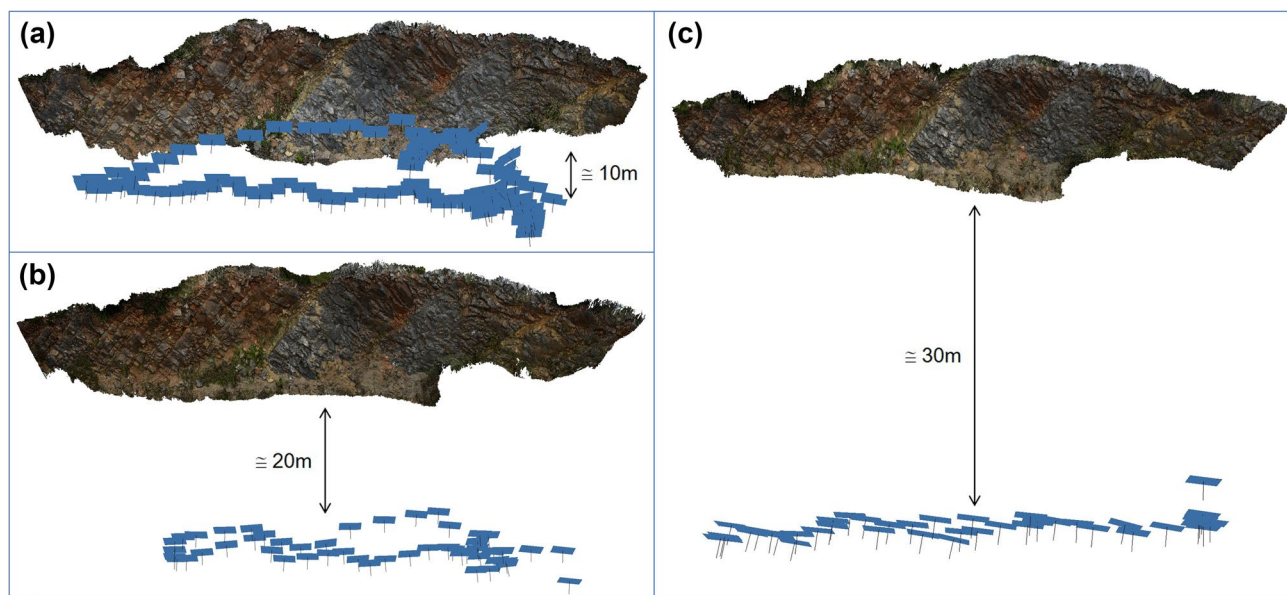


Fig. 5 Photogrammetric network design of the three manual UAV flights: 10 m distant from the slope (a), 20 m (b) and 30 m (c)



Fig. 6 Example of targets measured during the topographic survey for the UAV flights and TLS alignment and georeferencing

executed on the same day of fieldwork. TLS uses a laser beam (with wavelength varying between the visible and near infrared portion of the spectrum—1532 nm in this work) to measure the distance between a source point and a reflective surface, so as to create a 3D point cloud of surfaces and objects that fall within the field of view of the scanner.

In this study, the TLS survey was carried out using a Trimble™ TX8 device (specifications in Table 2). It is a pulse-based device that measures the time a laser pulse takes to travel from a source to a reflective surface and back again (round trip). Once the time is known, given that the velocity is equal to the speed of light, it is possible to calculate the distance between the source and the target. The instrument

has 360° horizontal and 317° vertical fields of view and must be firmly mounted on a tripod. To observe the surrounding environment as completely as possible, and to reduce shadows, three overlapping point clouds were acquired from different scan positions with a scanning spatial resolution set to 0.003 m at a distance of 15 m.

The topographic survey of artificial targets, performed by means of GNSS geodetic receivers and TS, allowed registration of the TLS point clouds with the necessary millimetric spatial accuracy and allowed georeferencing. The utilized targets, acting as physical constraints in the roto-translation of clouds, were the same as those described for the UAV exterior orientation. At least 5 targets were visible from each scan position, thereby limiting errors and improving spatial accuracy. The three point clouds were stored and processed using Trimble™ RealWorks software. During the field survey, after every scan, the device was alternated with a Nikon™ D7100 digital camera (see Table 2 for details), securely mounted on a Leica™ Nodal Ninja 3II, with the aim of acquiring high definition (HD) images. To obtain full panoramic images (360° view), photos were shot at pre-set angles with sufficient overlap with reference to the selected focal length (Table 2). Through use of a fisheye lens, only 6 photos (every 60°) were necessary to cover the whole panorama from a single position. Given the spherical view of TLS, only a fisheye lens camera can record the same field of view in one image. Therefore, the combination of a laser scanner and a hemi-spherical fisheye lens camera is essential.

Co-registration of TLS data and HD photos based on artificial markers and central perspective imagery can produce

highly accurate results (Kersten 2006). Since the photos were taken with a fisheye lens, the geometric model was adapted accordingly, as described in Schwalbe et al. (2009). As shown experimentally in Schneider and Schwalbe (2008), the integration of 3D point clouds with fisheye images yields equally precise results to that obtained with standard central perspective (Schmidt et al. 2012). Therefore, having the focal centre of the camera lens in correspondence with the optical centre of the scanner, the HD photos were processed and aligned (i.e. texture mapping) to the point clouds (Vanneschi et al. 2014; Mastrococco et al. 2018b). Photographs were handled using specific software for the creation of equirectangular images (PTGui™—New House Internet Services BV). After conversion to cube map images using Pano2QTVR Gui (Garden Gnome software™), they were aligned to the TLS point cloud. Using this methodology, a 3D photorealistic point cloud map suitable for photointerpretation and roughness amplitude measurement was created.

3.4 Roughness Profiles Acquisition

The bi-dimensional profiles of 25 discontinuities were collected by using both traditional profilometers during field investigation and in the laboratory by digitizing joint profiles directly from the processed point clouds. Four different scales were adopted, using profiles 10 cm, 30 cm, 60 cm and 100 cm long. As previously indicated, for the shorter lengths, the reference profiles were measured directly in the field by using two different profilometers, 10 cm and 30 cm long. The measured discontinuities were photographed, and the respective images imported into Autodesk™ AutoCad, scaled and vectorized. In addition, a white marker was used on the rock faces to highlight the location of the different profiles in such a way that they could be easily recognized on the point clouds.

In a second phase, new profiles for the same discontinuities (on the same exact location) were vectorized from the four different point clouds (UAV 10 m, 20 m, 30 m and TLS) within Leica™ Cyclone 9.0. Before vectorization, UAV and TLS point clouds were aligned by applying an Iterative Closest Point algorithm, within Trimble™ RealWorks software; the error obtained was about 3 mm (i.e. 3D quality) which was considered acceptable for the purposes of this work.

This procedure allowed verification of the quality of the colored TLS point cloud. The profile traces from Leica™ Cyclone 9.0 were then imported in Autodesk™ AutoCad. In this way, a total of 250 profiles were drawn (for 25 discontinuities, on each point cloud, for two different lengths of 10 cm and 30 cm). This approach allowed a direct comparison of the profiles digitized on the point clouds with those manually measured in the field.

As it was impossible to manually acquire longer profiles during the fieldwork, the remaining profile data (for the 60 cm and 100 cm long profiles) were collected using the TLS point cloud as a reference. Subsequently, a further 25 discontinuities were identified, and bi-dimensional profiles digitized within Leica™ Cyclone 9.0 on the four point clouds (UAV 10 m, 20 m, 30 m and TLS). Again, all the profiles were imported in Autodesk™ AutoCad for joint surface roughness amplitude comparisons. A total of 200 profiles were collected for the 60 cm and 100 cm scales. Overall, the Autodesk™ AutoCad measurements determined the length and the asperity amplitude of the 450 profiles, with the procedure summarized in Fig. 7.

To minimize the potential bias due to high observation angles, which may be possible for discontinuities located at the top of the slopes as TLS is a ground-based observation system, and to ensure direct comparison with the manual engineering-geological survey, only joints at the bottom of the outcrop were considered for roughness amplitude measurement and JRC determination.

To evaluate any potential bias in the work that has been performed, it is important to consider any scale-related effects associated with the length of the compared profiles. The working scale depends on the length of the surfaces determined in the field. A roughness value derived from a 10 cm profile can be used for evaluating at a laboratory specimen scale, but it may be insufficient for characterizing, in a reliable way, a joint surface several metres long. In addition, point cloud noise can have a different impact on the JRC determination depending on the used profile length: an error of 2 mm may cause a large difference in a 10 cm profile, while it may be negligible for a 100 cm long profile. To remove such bias, the method proposed by Barton (1982—Fig. 4) was adopted and different roughness amplitude measurements were executed on several different surface

Table 2 Utilised terrestrial laser scanner (TLS) and camera specifications

TLS	Range (m)	Scan rate (pts/sec)	Accuracy of single measurement (m) at 2 m–80 m, one sigma	Angular accuracy (horizontal/vertical- μ rad), one sigma	
Trimble TX8	340 m extended range upgrade @ 90% reflectivity	1,000,000	< 0.002 (distance)	80	
Camera	Sensor type	Sensor size (mm)	Image size (pixel)	Pixel size (mm)	Focal length (mm)
Nikon D7100	CMOS	23.50 × 15.60	6000 × 4000	0.0039	18.0

lengths. The chart represented in Fig. 4 was re-created in Microsoft™ Excel and the JRC values determined for every investigated profile length. Such an approach was utilized to minimize any subjective data analysis. The comparison between different profiles became purely geometrical (based on profile length and amplitude).

4 Results

4.1 Digital 3D Point Clouds from UAV and TLS Data

The alignment process of images from the UAV surveys resulted in re-projection errors of 0.41, 0.38 and 0.38 pixels for the 10 m, 20 m and 30 m flights, respectively, with a final root mean square error (RMSE) on GCPs of about 4 mm (details in Table 3). The final point clouds (Fig. 8) are made of more than 92,000,000, 22,000,000 and 10,000,000 points, respectively, for the 10 m, 20 m and 30 m flights, with a mean point spacing varying from 1 to 4 mm (UAV 10 m), 1 to 10 mm (UAV 20 m) and 2 to 20 mm (UAV 30 m).

Figure 9 shows the final TLS point cloud obtained following registration and processing of the three separate

scans. The RMSE of the registration process on targets was about 6 mm, with a final point cloud consisting of more than 100,000,000 points, with a mean point spacing varying from 1 to 4 mm.

Before starting the process of roughness amplitude measurement on profiles, an important consideration is made concerning the achieved RMSE from the registration process on targets. It represents the absolute georeferencing error. Geometrical validation of single profiles obtained from the point cloud data has been carried out by comparing them with the true discontinuity geometry acquired from traditional profilometers.

4.2 Roughness Amplitude Measurement on 10 cm Long Profiles

Figure 10 shows the comparison of the roughness amplitude measurements as derived from the 10 cm long profiles. The different symbols on the four graphs (rhombus for the UAV 10 m point cloud; square for the UAV 20 m point cloud; triangle for the UAV 30 m point cloud; circle for the TLS point cloud) indicate the amplitude values measured on each profile (for a total of 25 profiles). The vertical bars

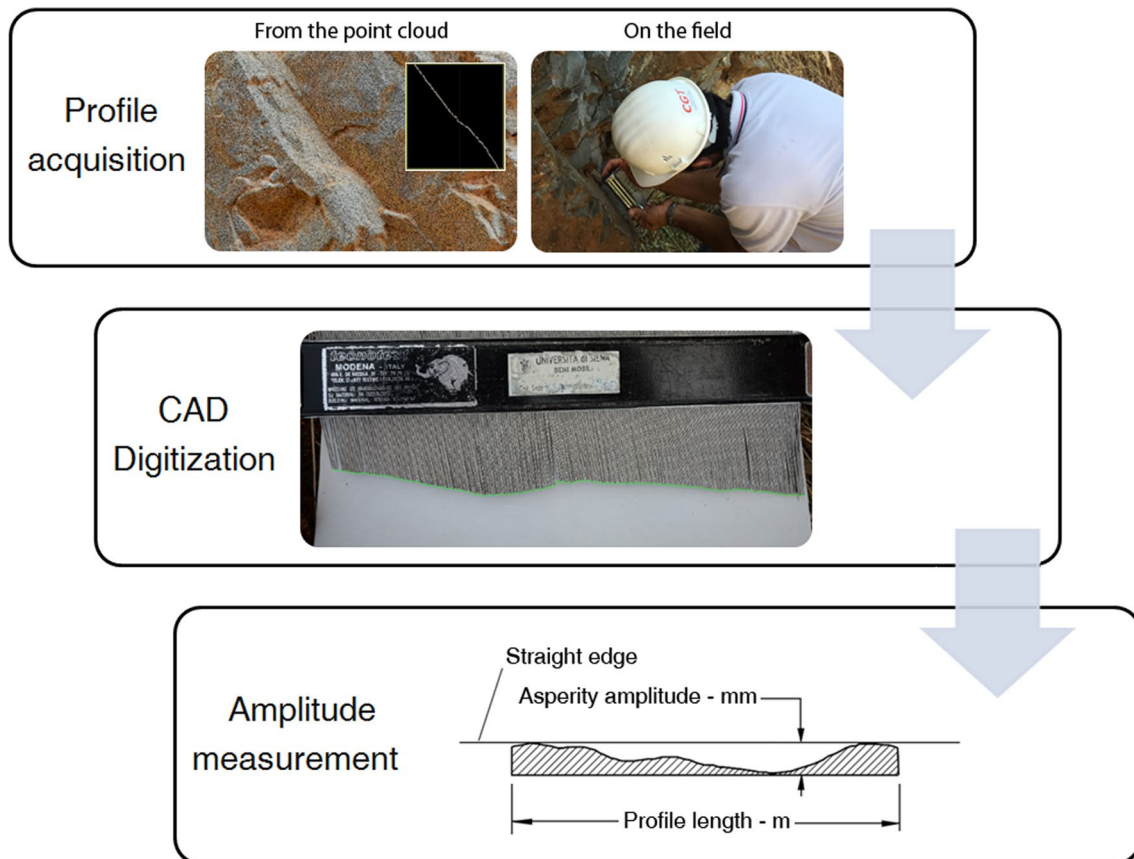


Fig. 7 Graphical summary of methods used to measure the joint surface roughness amplitude

represent the difference with respect to the real amplitude value, measured during fieldwork with the profilometer. As an example, profile number 5 on the UAV 20 m point cloud shows an amplitude of 6.4 mm, while the real value, measured during fieldwork on the profile location, is 2.2 mm; this difference is represented on the graph by a vertical bar pointing downward.

Results suggest that measurements obtained from UAV 10 m and TLS show the best fit when compared to direct field observations, while lower accuracy is observed from measurements derived from the UAV 20 m and UAV 30 m surveys. In particular, the RMSE of measurements on the TLS and the UAV 10 m point clouds is about 3 mm, while for observations executed on the UAV 20 m and the UAV 30 m point clouds are 5 mm and 11 mm, respectively.

Table 3 Information for the photogrammetric surveys and subsequent processing

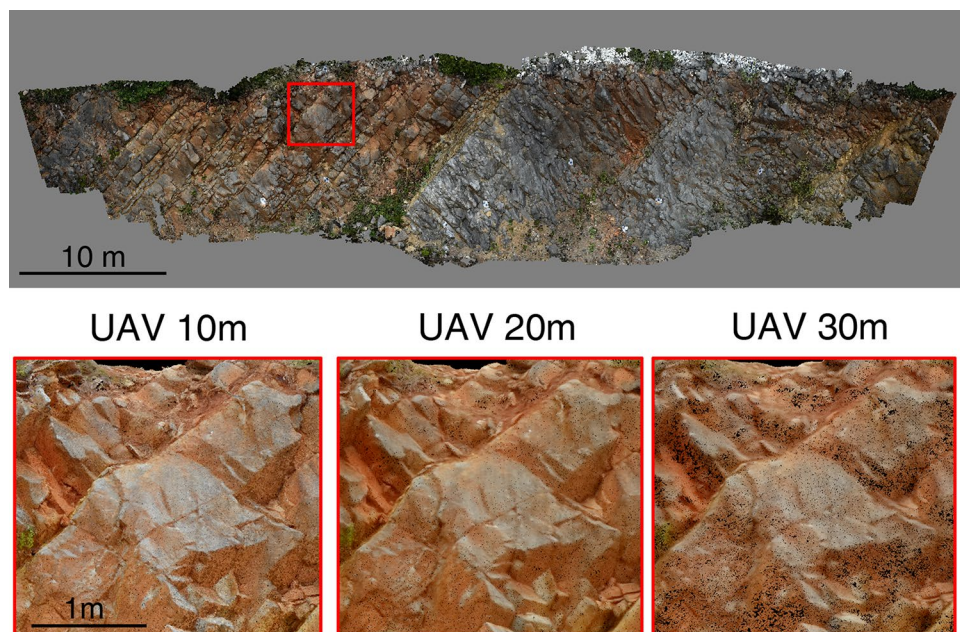
Average flying distance from the slope	10 m	20 m	30 m
Number of images	98	51	40
Average GSD ^a	2.5 mm/pixel	5.4 mm/pixel	7.5 mm/pixel
# Tie Point	25,849	13,347	11,721
GCP ^b RMSE ^c	3.9 mm	4.5 mm	3.9 mm
GCP reprojection error	0.41 pixel	0.38 pixel	0.38 pixel

^aGround sample distance

^bGround control point

^cRoot mean square error

Fig. 8 Example of a point cloud from the UAV survey representing the whole slope under study (top); details of single point clouds as obtained from the 10 m, 20 m and 30 m distant flights (bottom)



4.3 Roughness Amplitude Measurement on 30 cm Long Profiles

Results of roughness amplitude measurement comparisons, related to the 30 cm long profiles, are illustrated in Fig. 11. The different symbols of the four graphs, as described for Fig. 10, indicate the amplitude values measured on each profile (for a total of 25 profiles). Similarly, when compared to the previous analysis, results show how measurements obtained from UAV 10 m and TLS present a better fit when compared to the field-derived values, with RMSEs of about 3 mm. RMSEs of measurements on the UAV 20 m and the UAV 30 m point clouds, compared to the real values from fieldwork, are 5.5 mm and 12 mm, respectively.

4.4 Roughness Amplitude Measurement on 60 cm Long Profiles

Given the unavailability of a 60 cm long profilometer, it was decided to use the profiles obtained from TLS as reference for the comparison with measurements derived from the UAV point clouds. This choice is supported by the documented evidence that TLS point clouds have already been successfully used by several authors for obtaining roughness parameters from rock discontinuities. Furthermore, instead of the roughness amplitude, JRC values derived from TLS and UAV point clouds were compared with each other. The difference in amplitude values is expected to remain essentially constant with the increase of the profile length, apart from the fact that a longer profile has a higher probability of containing errors on the point cloud data. A given difference in amplitude, 2 mm for example, has a different influence on



Fig. 9 TLS point cloud representing the whole slope under study (top); the three different scan positions are highlighted (triangles). Details of the point cloud (bottom)

the final JRC value depending on the profile length because of the “scale effect”. Following the Barton method (1982—Fig. 4), a 2 mm amplitude difference in a 10 cm long profile may result in a JRC difference of 8 points, while the same 2 mm difference in a 60 cm long profile may result in a JRC difference of only 2 points. Therefore, JRC values were used to compare the accuracy of TLS and UAV roughness amplitude measurements.

To establish the level of accuracy of the TLS point cloud chosen for the roughness estimation, JRCs from the 10 cm and 30 cm long profiles were calculated by using the chart shown in Fig. 4. The values (calculated on a spreadsheet together with those from UAV point clouds) were then compared with corresponding values determined with the profilometer during fieldwork, and RMSEs calculated (Fig. 12).

Results shown in Fig. 12 show that the smallest JRC RMSEs were detected for the TLS point cloud both on the 10 cm and the 30 cm long profiles. Except from the JRC RMSEs of the UAV 30 m point cloud, there is a general trend of RMSE reduction when the analysis moves from 10 to 30 cm long profiles. In the case of TLS, the RMSE decreases from 4 to 2.2 points for the 10 cm and the 30 cm profiles, respectively. Given the registered trend, it can be reasonably hypothesized that, in agreement with the Barton

(1982) method, the JRC RMSE would drop below 2 points for the 60 cm long profiles; this is possible because of the “scale effect”—as length increases there is reduced influence of the point cloud noise on JRC determinations. It should also be remembered that the traditional field determinations of JRC are generally referred to 10 standard profiles (as proposed by Barton and Choubey 1977), where every profile is related to a JRC class ranging within a difference of 2 points. This means that JRC field estimation is based on subjective judgement for differences lower than 2 points. Based on this, the following criterion was adopted: a difference of JRC value lower than 2 points can be considered acceptable, since it provides the same accuracy level of traditional field determinations.

For completeness, Fig. 13 shows the comparison values of roughness amplitude measurements determined for 60 cm long profiles obtained from UAV 10 m, UAV 20 m and UAV 30 m with respect to TLS point cloud.

As with previous analyses, results indicate that measurements obtained from UAV 10 m point cloud show the best correspondence with respect to measurements performed on the TLS point cloud, with a RMSE of 3 mm. RMSEs of measurements taken on the UAV 20 m and the UAV 30 m

Fig. 10 Graphs resulting from the measurement of roughness amplitude on the 10 cm long profiles. Different symbols (rhombus for the UAV 10 m point cloud; square for the UAV 20 m point cloud; triangle for the UAV 30 m point cloud; circle for the TLS point cloud) indicate the amplitude values measured on each profile (for a total of 25 profiles). Vertical bars represent the difference with respect to the real amplitude value, measured during fieldwork with the profilometer

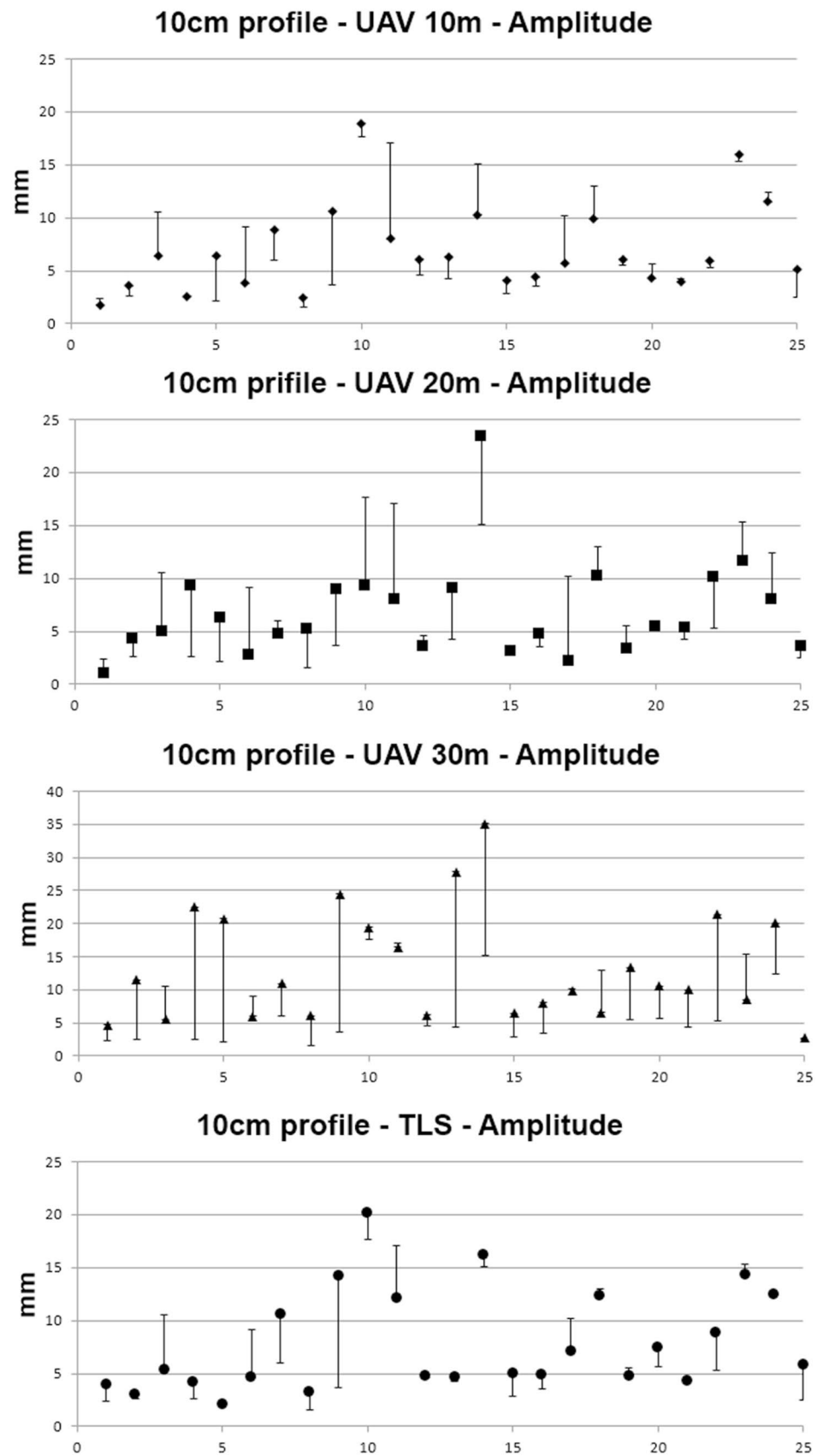
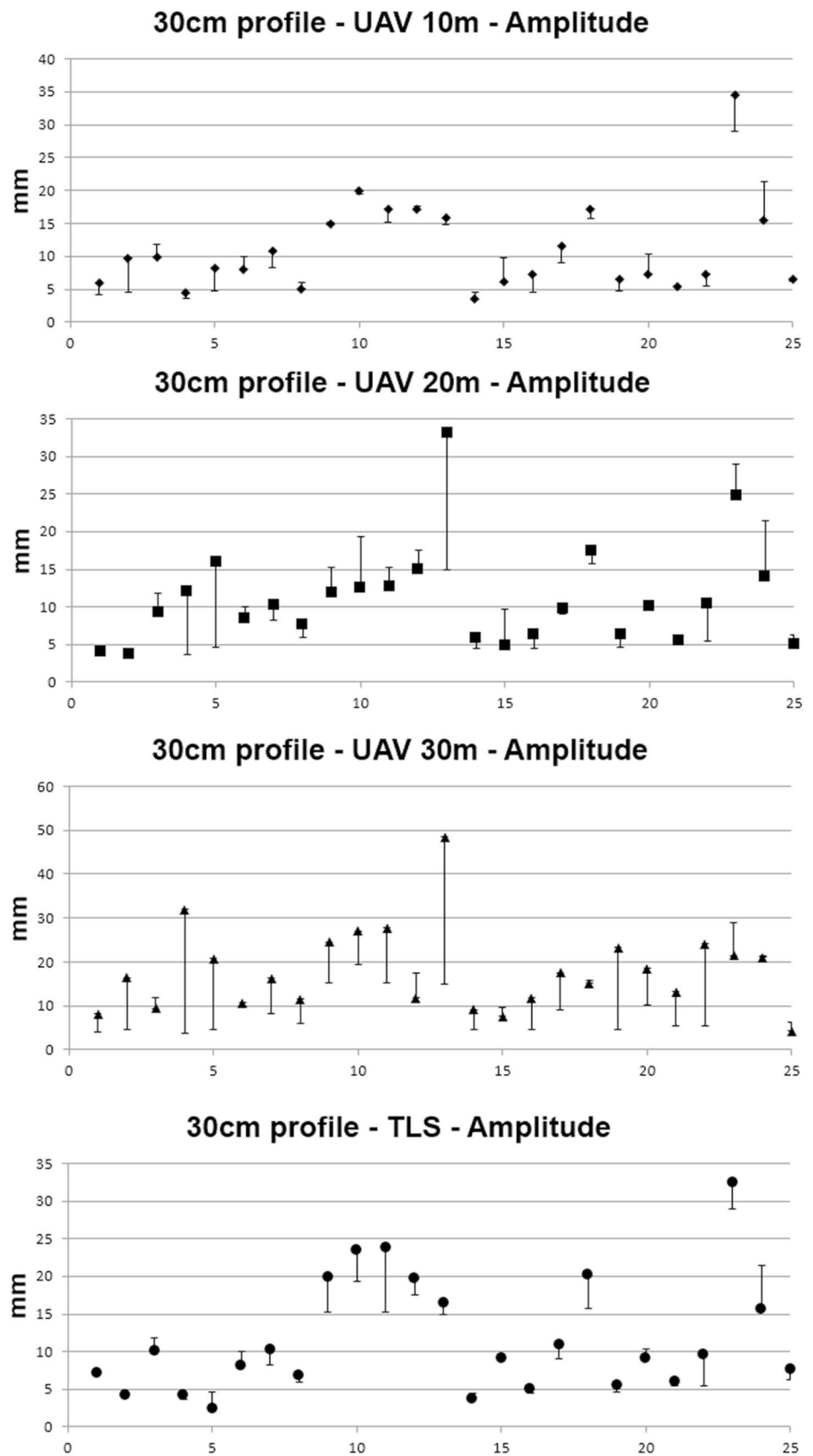


Fig. 11 Comparison of roughness amplitude measurements on 30 cm long profiles as obtained from UAV 10 m, UAV 20 m, UAV 30 m and TLS with respect to the roughness amplitude values derived from fieldwork



point clouds, compared to values derived from TLS, are 5 mm and 9 mm, respectively.

4.5 Roughness Amplitude Measurement on 100 cm Long Profiles

Results of roughness amplitude measurement comparisons, related to 25 profiles, 100 cm long, for every UAV point cloud (as derived from flights 10 m, 20 m and 30 m distant from the slope) are illustrated in Fig. 14. Once more, roughness amplitude measurements derived from the UAV 10 m point cloud show the best correspondence with respect to that from TLS, with a RMSE of 4 mm. In this case, RMSEs of measurements executed on the UAV 20 m and the UAV 30 m point clouds, compared to values derived from TLS, are 6 mm and 9 mm, respectively.

4.6 Qualitative Assessment of JRCs Derived from the Analysis of Different Point Clouds

Based on evidence from previous figures (Figs. 10, 11, 12, 13 and 14), roughness amplitude measurements carried out on the UAV 10 m profiles are very close to those derived from TLS for all the different profile lengths. As expected, these show the highest correspondence when compared to fieldwork data from the profilometer. Profiles derived from UAV 20 m and 30 m point clouds show higher differences. Since amplitude measurements obtained from profiles of different length (i.e. 60 cm and 100 cm) cannot be directly compared, to remove the scale bias, a qualitative assessment of JRCs obtained from the different point clouds was performed by using the Barton (1982) method. RMSEs were then determined using the JRC as term of reference. For the 10 cm and 30 cm long profiles, RMSE was calculated with respect to JRC values determined during fieldwork from profilometers, while for the 60 cm and 100 cm long profiles, RMSE was calculated with respect to JRC derived from TLS profile analyses. Figure 15 shows the results of such an analysis.

Figure 15 shows how significant differences (> 4 JRC points) are obtained when considering the 10 cm long profiles compared to values determined from fieldwork. When considering the 30 cm long profiles, results from the TLS point cloud differ from field determinations by only 2 points, while RMSE values are higher for the respective UAV flights. If the observed scale length is increased to 60 cm, results from the UAV 10 m point cloud are very close to that resulting from the TLS point cloud. Acceptable values of difference (< 2 JRC points) can also result from the UAV 20 m point clouds when adopting 100 cm long profiles. As for the UAV 30 m point cloud, an acceptable level of accuracy is never reached for the investigated scale lengths.

5 Discussion

The case study aimed to establish whether UAV image acquisition, coupled with SfM–MVS techniques, can be considered a reliable approach to measure the discontinuity surface roughness and the relative JRCs under field conditions. Importantly, the UAV method has allowed comparison of surface profiles across different roughness length scales with a range varying from 0.1 to 1 m and has overcome data acquisition difficulties related to shadow-zone presence in both the horizontal and vertical directions.

To obtain accurate and georeferenced 3D point clouds, Salvini et al. (2018) emphasized how careful execution of the UAV photogrammetric survey plays a crucial role in providing accurate results necessary for subsequent analyses. This is also critical for discontinuity roughness evaluation.

With this in mind, the following guidelines are considered essential: (i) depending on the regulations in force in the country where the investigation takes place, a pilot with a UAV flight license is required, as well as the authorization of the Entity/Company, (ii) the drone used

Fig. 12 RMSEs of JRCs calculated on the 10 cm and 30 cm long profiles, derived from TLS, UAV 10 m, UAV 20 m, UAV 30 m point clouds, with respect to JRCs determined with profilometer during fieldwork

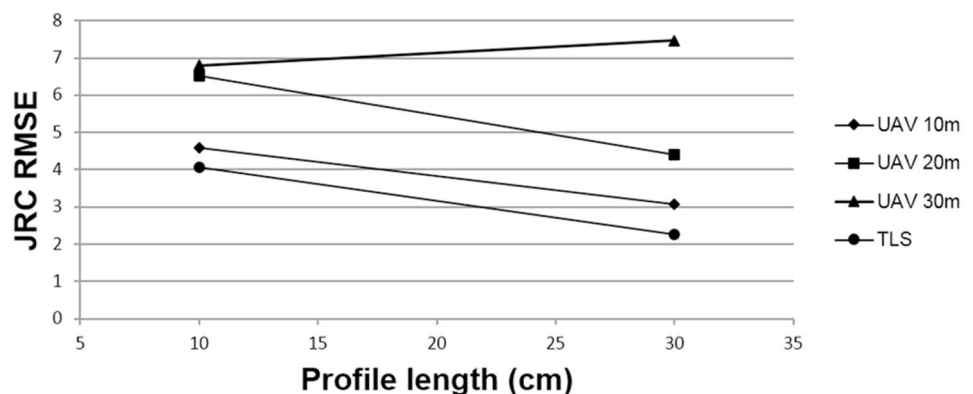
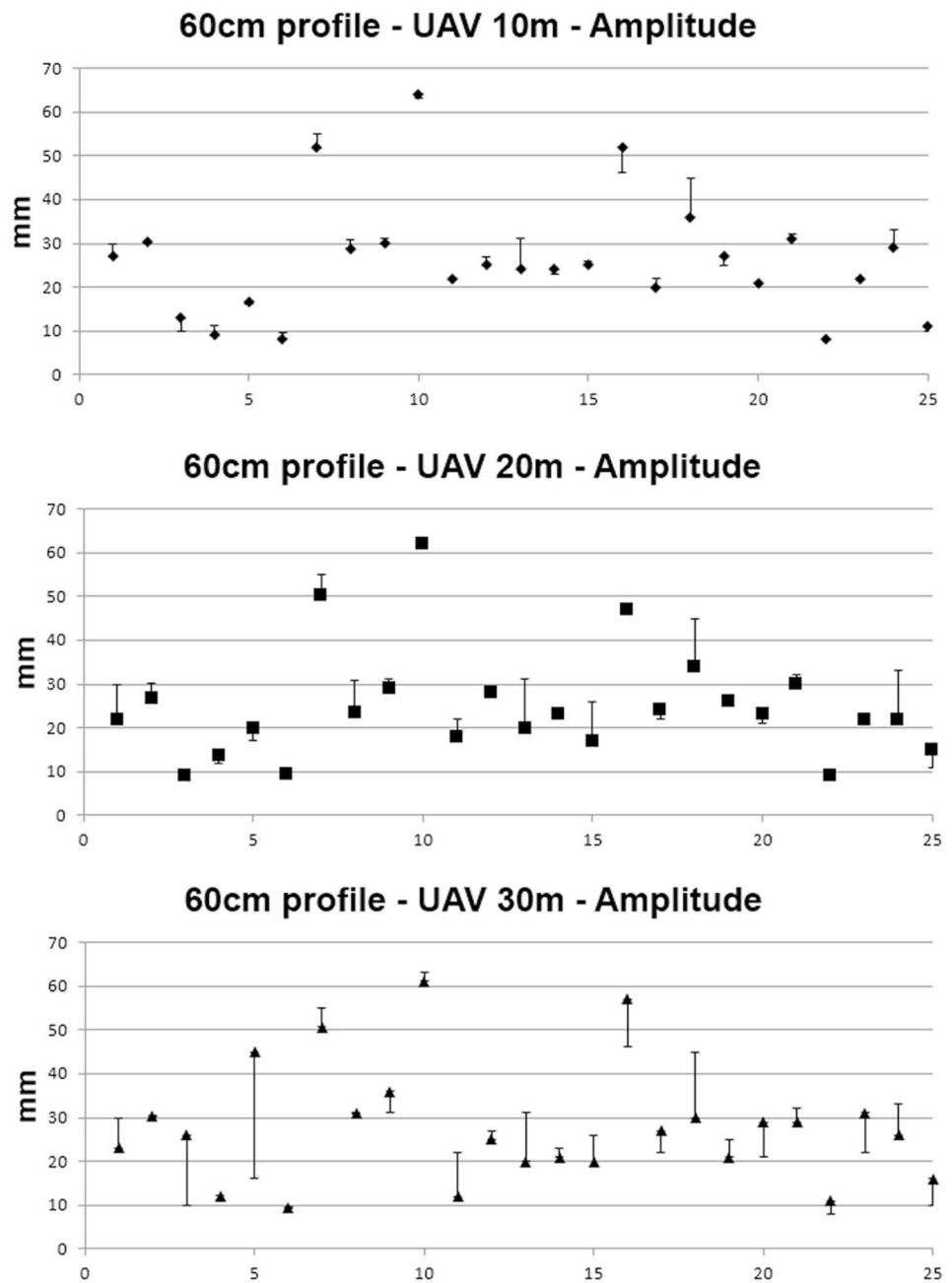


Fig. 13 Comparison of roughness amplitude measurements on 60 cm long profiles as obtained from UAV 10 m, UAV 20 m and UAV 30 m with respect to TLS point cloud



must be stable and easily manoeuvrable, (iii) unfavourable weather conditions (e.g. wind, fog, snow) should be absent, (iv) image quality must be high (e.g. digital camera with minimum 16 MPix or higher resolution, no ultra-wide angle and fisheye lenses) as well as imagery redundancy (minimum 60% and 80% of sidelap and overlap, respectively). Knowledge of camera calibration parameters is essential, and a robust network geometry of images acquisition needed, (v) the topographic survey of several GCPs and check points on the slope must be accurate and performed with GNSS and TS. The control points must be

spatially well distributed and correctly measured to avoid any nonlinear deformations of point cloud derived from SfM-MVS, (vi) very high-density point clouds must be produced, and this requires high-performance PCs and graphic cards, (vii) it is always necessary to compare and validate the derived data with those from ground measurements in the same location (perhaps by marking them on the outcrop). In this sense, profiles must be photographed on the ground and digitized for analytical comparison.

Using these guidelines, data from UAV surveys have provided accurate 3D point clouds from which engineering-geological parameters necessary for the

Fig. 14 Comparison of roughness amplitude measurements on 1 m long profiles as obtained from UAV 10 m, UAV 20 m and UAV 30 m with respect to TLS point cloud

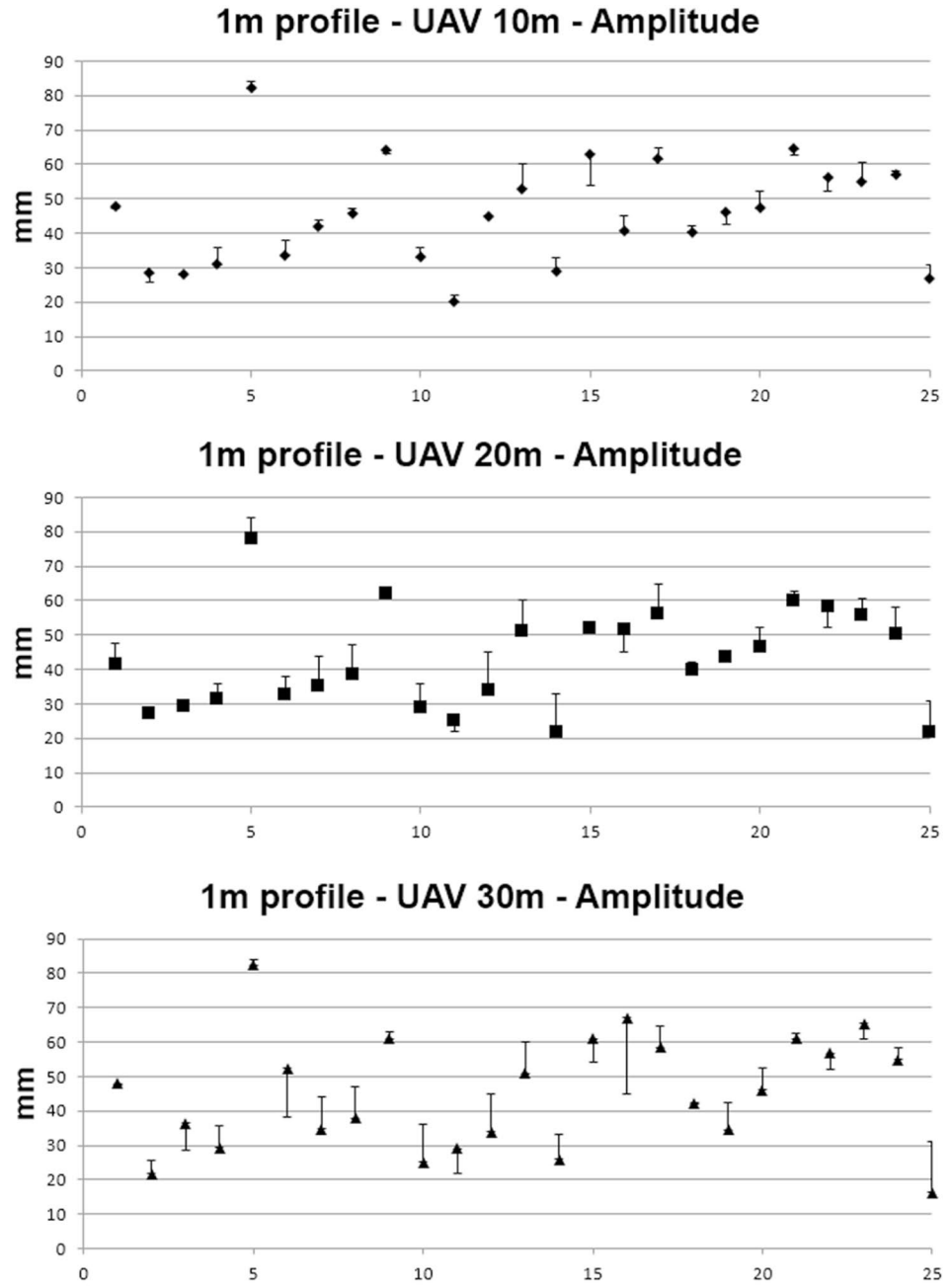
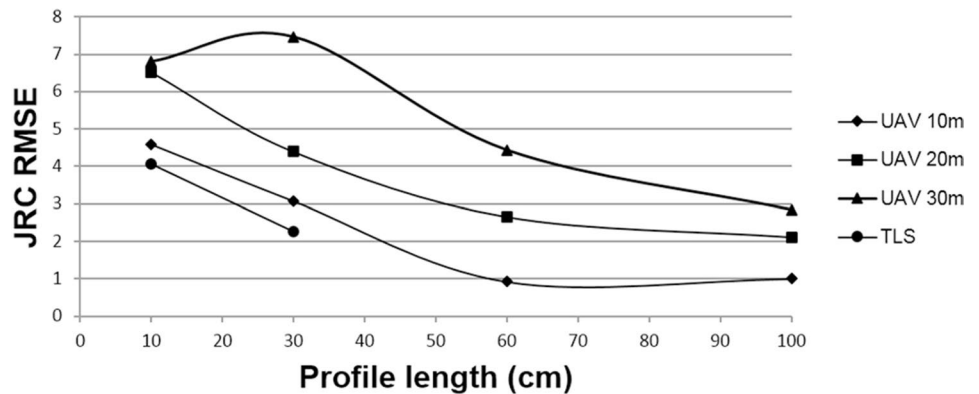


Fig. 15 RMSEs of JRCs: for the 10 cm and 30 cm long profiles RMSEs of TLS, UAV 10 m, UAV 20 m, UAV 30 m point clouds are calculated in respect to JRCs determined with profilometers during fieldwork; for the 60 cm and 100 cm long profiles RMSEs of UAV 10 m, UAV 20 m, UAV 30 m point clouds are calculated with respect to JRCs measured from the TLS point cloud



characterization of a rock mass have been measured and compared to data directly measured during a comparative field survey. The results of the investigation demonstrate that it is possible to measure the roughness amplitude of rock discontinuities by using UAV point clouds acquired in a real geological environment. Nevertheless, it must be considered that the noise in the point cloud and the scale of analysis can have a significant impact on the measurement of roughness amplitude and in the determination of JRC value. The resultant point cloud noise and when using small scale for characterization (i.e. typically 10 cm) can result in significant differences in the JRC values produced. Results from this work demonstrates that these differences can be negligible if longer discontinuities are considered (i.e. 100 cm).

From the analysis of the 10 cm long profiles (Figs. 10, 11, 12, 13, 14 and 15), it can be observed how the best results are obtained for the amplitude measurements performed on the UAV 10 m and TLS point clouds. A RMSE of about 3 mm was calculated for both the UAV 10 m and TLS profiles with respect to the roughness amplitude directly measured with the profilometer. In terms of JRC, determined by using the chart shown in Fig. 4, this amplitude difference on a 10 cm long profile can cause a difference of 4.5 points. From this result it can be observed that a UAV flight correctly executed with stability and safety, close to the rock mass in such a way as to obtain a GSD of about 2.5 mm, can be used to produce a point cloud with an accuracy comparable to that of TLS. Nevertheless, results from 10 cm long profile presents errors that are too large for providing reliable results at a slope scale: the noise of the point cloud can cause millimetric differences in the amplitude measurements that, according to Barton (1982), lead to important differences in terms of JRCs. The analysis of the 10 cm long profiles derived from the UAV 20 m and UAV 30 m point clouds revealed, as expected, higher RMSEs with respect to the roughness amplitude measured with the profilometer during field survey. A RMSE of about 10 mm was calculated for the UAV 20 m profiles, while a RMSE of about 11 mm was calculated for the UAV 30 m profiles. In terms of JRC, these RMSEs can cause differences of 6.5 and 6.8 points, respectively. From Figs. 10, 11, 13 and 14 it can also be observed how profiles obtained from the UAV 30 m point cloud show errors due to high noise in the point cloud which were produced from the most distant UAV flight giving a GSD of about 7.5 mm.

For the 30 cm long roughness profiles, the best results were obtained for the amplitude measurements performed on the UAV 10 m and TLS point clouds. A RMSE of about 3 mm was calculated for both the UAV 10 m and TLS profiles with respect to the roughness amplitude directly measured with the profilometer. The observed amplitude variations cause JRC differences of about 3 points and 2.2 points

for the UAV 10 m profiles and the TLS profiles, respectively. From this result it can be noted that: (i) a similar UAV flight can give results comparable to that from a TLS survey, (ii) the noise of the point cloud on 30 cm long profiles has a lower effect in terms of JRC differences. The analysis of 30 cm long profiles derived from the UAV 20 m and UAV 30 m point clouds revealed, as expected, higher RMSEs with respect to the roughness amplitude measured with the profilometer during the field survey. RMSEs of about 5.5 mm and 12 mm were calculated for the UAV 20 m profiles and for the UAV 30 m profiles, respectively. In terms of JRC, these RMSEs cause differences of 4.4 and 7.5 points, respectively. Even at this scale, it can also be observed how the profiles obtained from the UAV 30 m point cloud show high positive errors.

The analysis of the 60 cm long profiles required a different reference profile; given the unavailability of profilometers of such a length, it was decided to use the roughness profiles derived from the TLS as the reference to be compared with data from UAV flights. Figure 12 show how the smallest difference, calculated on JRC values in respect to fieldwork data, were achieved for profiles derived from the TLS point cloud. The trend analysis revealed that the RMSE drops below 2, an acceptable value in terms of JRC accuracy, for the 60 cm long profiles. Figures 10, 11, 12, 13, 14 and 15 show that the best RMSEs were obtained again for amplitude measurements performed on the UAV 10 m with a RMSE of 3 mm. In terms of JRC, this amplitude variation can determine a difference lower than 1 point. These results confirm that a UAV flight, fully executed in a proper way, can provide results comparable to that from TLS. As for the roughness amplitude measurements on the 30 cm tests, achieved RMSEs indicate how the longer profiles provide lower JRC differences. The analysis of profiles derived from UAV 20 m and UAV 30 m point clouds revealed, once more, higher RMSEs. RMSEs of about 5 mm and about 9 mm were calculated for the UAV 20 m profiles and the UAV 30 m profiles, respectively; in terms of JRC, these RMSEs cause differences of 2.6 and 4.4 points. When the length of the analysed profile is 60 cm, the profiles obtained from the UAV 30 m point cloud show random negative and positive errors.

Lastly, results from the 100 cm long profiles (Figs. 10, 11, 12, 13, 14 and 15) confirm how the most accurate measurements were performed on the UAV 10 m point cloud with a RMSE of 4 mm (calculated with respect to the TLS point cloud) corresponding to a JRC difference of 1 point. The analysis of profiles derived from UAV 20 m and UAV 30 m point clouds show RMSEs on the amplitude measurements of about 6 mm and 8.5 mm, respectively. In terms of JRC, these RMSEs result in differences of 2.1 and 2.8 points, respectively.

Tables 4 and 5 provide a summary of the results. Table 4 shows the RMSEs of JRCs derived from UAV and TLS point

clouds compared to data directly collected with the profilometer during the field survey. Table 5 shows the RMSEs of JRCs derived from UAV point clouds compared to that from the TLS point cloud.

From the analysis of results, it can be concluded that a point cloud obtained from images with a GSD of about 2.5 mm (obtained in the present configuration with an UAV flight 10 m distant from the rocky slope) provides measurements of roughness amplitude comparable to that determined during a conventional field survey and that achievable from a TLS survey carried out from a similar distance. Nevertheless, the quality of the photogrammetry-based point cloud was not accurate enough to obtain reliable JRC values on a 10 cm long scale. On a 30 cm long roughness scale, JRCs obtained from profiles digitalized on the TLS point cloud show a RMSE of 2.2 point which is practically equal to the accuracy reachable in the field, with traditional hand mapping, based on subjective judgement for differences lower than 2 JRC points. This result confirms that the TLS point cloud, if accurately acquired and processed, may be used for JRC determination on rock discontinuities longer than 30 cm. For the same lengths, the measurements obtained from the UAV 10 m point cloud show a JRC RMSE of 3 points, only 1 point above the required reference accuracy.

When dealing with 60 cm long roughness profiles, the UAV 10 m point cloud provides JRCs comparable to those derived from the TLS point cloud, with an RMS error of about 1 point. The UAV 20 m flight, characterized by images with a GSD of about 5.5 mm, provides acceptable results (still considering a JRC RMSE of 2 as adequate) only on a 100 cm long scale. The UAV flight performed at about 30 m from the rock face, with a corresponding GSD of about 7.5 mm in this work, does not permit the necessary level of accuracy at any investigated scale. Probably, the higher errors identified for the 20 m and 30 m UAV point cloud are mainly due to the constant focal length used during the survey, which resulted in different GSD for the three point clouds. The higher the distance from the rock face, the bigger the GSD and less dense the point cloud (i.e. 92,000,000, 22,000,000 and 10,000,000 points for 10 m, 20 m and 30 m, respectively). From a less dense point cloud a less detailed profile of amplitude can be derived, with higher differences in respect to both the reference linear profiles as obtained using profilometer, and the TLS point cloud which, at equal distance from the exposed rock surfaces has a uniform point density.

The analysis of the RMSE trend suggests that it is possible to obtain reliable JRCs on longer profiles, but this should be further investigated on different case studies with larger exposures of (wider and longer) rock discontinuities.

Finally, it should be emphasized that the presented work is an attempt to evaluate the possibility of obtaining JRC values on inaccessible areas characterised by high and steep

Table 4 RMSE for JRCs calculated from different point clouds on profiles 10 cm and 30 cm long, compared to data directly collected with the profilometer during the field survey

Profile length (cm)	JRC RMSE			
	TLS	UAV 10 m	UAV 20 m	UAV 30 m
10	4	4.5	6.5	6.8
30	2.2	3	4.4	7.5

Table 5 RMSE for JRCs calculated from different point clouds on profiles 60 cm and 100 cm long, compared to that from the TLS point cloud

Profile length (cm)	JRC RMSE		
	UAV 10 m	UAV 20 m	UAV 30 m
60	0.9	2.6	4.4
100	1	2.1	2.8

natural or artificial slopes. The test work was not performed with the aim of obtaining “exact JRC values”, which are fundamental in shear strength determination. Even considering the rapid development in technology, it is still impossible to obtain “exact” JRCs from digital point clouds in open-field conditions. It may be possible to reach high accuracy levels in a controlled environment, as the case of a laboratory, but this is not possible in a real geological context, where problems arise in terms of light, UAV stability, accessibility, wind, etcetera. This investigation was devised as an attempt to verify if, using a commercial equipment (e.g. compact digital camera, multirotor UAV), it was possible to determine JRCs with an accuracy similar to that usually obtainable in the field by using a traditional profilometer. As Poropat (2008) discussed the acquisition and use of point cloud data for joint roughness measurement should be undertaken with due consideration of the accuracy, resolution and precision of the data.

It is important to undertake similar work for different lithologies, to further explore the possibility to adopt JRC determination (acquired by using different methods) from UAV systems as common practice in engineering geology.

6 Conclusions

Results from the presented work confirm that 3D digital point clouds derived from terrestrial laser scanning (TLS) are very detailed and, through correct processing, can be used to carry out discontinuity roughness amplitude measurement and subsequent determination of the Joint Roughness Coefficient (JRC). This data has proven to be comparable to joint roughness determinations carried out during

conventional field surveys with traditional profilometers. In this paper, we have compared the use of these proven methodologies with 3D points clouds generated from UAV flights executed at short distances from a rocky slope made of calcarenites. In particular, the results from UAV flights have been presented showing evaluation of joint roughness amplitude measurement and JRC determination using 3D digital point clouds generated from image processing of UAV flights at varying distances from the rock slopes (10 m, 20 m and 30 m).

The data analysis included the measurement of four different roughness profile lengths: 10 cm, 30 cm, 60 cm and 100 cm. Comparisons between the different profiles determined for specific discontinuities have been presented, in terms of RMSE, with respect to JRC values determined during fieldwork from profilometers for the 10 cm and 30 cm long profiles. For roughness profiles 60 cm and 100 cm long, the RMSEs were calculated with respect to JRCs derived from the analysis of TLS point cloud.

Results from the investigation confirm that it is possible to measuring the roughness amplitude of rock discontinuities by using UAV point clouds acquired under typical field conditions if best practice guidelines are followed. From the analysis of the 10 cm long roughness profiles the best results are obtained for the amplitude measurements performed on the UAV 10 m and TLS point clouds. The roughness amplitude measurements carried out on the UAV 10 m profiles are very close to the level of accuracy achieved when using a TLS for all the different profile lengths. Results of the investigation show that when the imagery ground sample distance (GSD) is lower than 3 mm, reliable JRCs may only be calculated on discontinuities of profile lengths greater than 60 cm. For higher GSD (more than 5 mm) the computed JRCs results are only reliable on a roughness scale of 100 cm or longer.

The results verify the possibility of obtaining JRCs with a level of accuracy comparable to those commonly accepted in direct engineering-geological surveys through use of a conventional profilometer. This work provides an improved understanding of the use of remotely captured data for discontinuity characterization in engineering-geological investigations and provide evidence for confidence in their use for such purposes. Results from this specific research demonstrate that 3D digital point clouds, as derived from the processing of drone-flight images, have been successfully used for reliable representation of discontinuity joint roughness for profiles longer than 60 cm, whereas conventional engineering-geological surveys are still necessary for evaluation of JRC at classical scales (10–30 cm). Nevertheless, Authors wish to underline that the minimum length of any profile is dependent on several factors including, but not limited to, the resolution of

the camera, the accuracy of the exterior orientation, the outcrop exposition, the type of rock, etcetera. Therefore, given the importance and the deep complexity of the topic further investigation are desirable in future.

References

- Agisoft (2016) Agisoft Photoscan user manual professional edition, version 1.2.5. Agisoft. https://www.agisoft.com/pdf/photoscan-pro_1_2_5_en.pdf. Accessed 20 Apr 2020
- Assali P, Grussenmeyer P, Villemin T et al (2014) Surveying and modeling of rock discontinuities by terrestrial laser scanning and photogrammetry: semi-automatic approaches for linear outcrop inspection. *J Struct Geol* 66:102–114. <https://doi.org/10.1016/j.jsg.2014.05.014>
- Baker BR, Gessner K, Holden E-J, Squelch AP (2008) Automatic detection of anisotropic features on rock surfaces. *Geosphere* 4:418–428. <https://doi.org/10.1130/ges00145.1>
- Barton N (1973) Review of a new shear-strength criterion for rock joints. *Eng Geol* 7:287–332. [https://doi.org/10.1016/0013-7952\(73\)90013-6](https://doi.org/10.1016/0013-7952(73)90013-6)
- Barton N (1982) Modelling rock joint behaviour from in situ block tests: implications for nuclear waste repository design. Technical Report, Terra Tek, Inc., Salt Lake City, United States
- Barton N, Choubey V (1977) The shear strength of rock joints in theory and practice. *Rock Mech Felsmechanik Mécanique des Roches* 10:1–54. <https://doi.org/10.1007/BF01261801>
- Bitenc M, Scott Kieffer D, Khoshelham K, Vežočanik R (2015) Quantification of rock joint roughness using terrestrial laser scanning. In: *Engineering Geology for Society and Territory—Volume 6: applied geology for major engineering projects*, pp 835–838
- Bonini M (1999) Basement-controlled Neogene polyphase cover thrusting and basin development along the Chianti Mountains ridge (Northern Apennines, Italy). *Geol Mag* 136:133–152. <https://doi.org/10.1017/S0016756899002277>
- Bortolotti V, Passerini P, Sagri M, Sestini G (1970) The miogeosynclinal sequences. *Sediment Geol* 4:341–444. [https://doi.org/10.1016/0037-0738\(70\)90019-9](https://doi.org/10.1016/0037-0738(70)90019-9)
- Bretar F, Arab-Sedze M, Champion J et al (2013) An advanced photogrammetric method to measure surface roughness: application to volcanic terrains in the Piton de la Fournaise, Reunion Island. *Remote Sens Environ* 135:1–11. <https://doi.org/10.1016/j.rse.2013.03.026>
- Canuti P, Focardi P, Sestini G (1965) Stratigrafia, correlazione e genesi degli scisti policromi dei monti del Chianti (Toscana). *Boll Soc Geol Ital* 84(6):93–166
- Colomina I, Molina P (2014) Unmanned aerial systems for photogrammetry and remote sensing: a review. *ISPRS J Photogramm Remote Sens* 92:79–97. <https://doi.org/10.1016/j.isprsjprs.2014.02.013>
- Corradetti A, McCaffrey K, De Paola N, Tavani S (2017) Evaluating roughness scaling properties of natural active fault surfaces by means of multi-view photogrammetry. *Tectonophysics* 717:599–606. <https://doi.org/10.1016/j.tecto.2017.08.023>
- Deliormanli AH, Maerz NH, Otoo J (2014) Using terrestrial 3D laser scanning and optical methods to determine orientations of discontinuities at a granite quarry. *Int J Rock Mech Min Sci* 66:41–48. <https://doi.org/10.1016/j.ijrmms.2013.12.007>
- Elter FM, Sandrelli F (1994) Inquadramento strutturale dei Monti del Chianti. *Boll della Soc Geol Ital* 114:537–547
- Fan W, Cao P (2019) A new 3D JRC calculation method of rock joint based on laboratory-scale morphology testing and its

- application in shear strength analysis. *Bull Eng Geol Environ.* <https://doi.org/10.1007/s10064-019-01569-0>
- Fazzuoli M, Pandeli E, Sani F (1994) Considerations on the sedimentary and structural evolution of the Tuscan Domain since early Liassic to Tortonian. In: Proceedings of the 76th summer meeting of the Societa Geologica Italiana; The Northern Apennines; Part 1, The Tuscan Nappe, the ophiolitic sequences, the turbiditic successions, pp 31–50
- Fazzuoli M, Pandeli E, Sandrelli F (1996) Nuovi dati litostratigrafici sulla Scaglia Toscana (Scisti Policromi) dei Monti del Chianti (Appennino Settentrionale). *Atti Soc Toscana di Sci Nat* 103:95–104
- Fazzuoli M, Pandeli E, Sandrelli F (2004) The Mesozoic to tertiary succession of the Northern Monti del Chianti: recent stratigraphic and tectonic advances. In: D M, P B (eds) The “Regione Toscana” Project of Geological Mapping: Case histories and data acquisition. Regione Toscana, Servizio Geologico Regionale, pp 187–198
- Feng Q, Fardin N, Jing L, Stephansson O (2003) A new method for in situ non-contact roughness measurement of large rock fracture surfaces. *Rock Mech Rock Eng* 36:3–25. <https://doi.org/10.1007/s00603-002-0033-1>
- Firpo G, Salvini R, Francioni M, Ranjith PG (2011) Use of digital terrestrial photogrammetry in rocky slope stability analysis by distinct elements numerical methods. *Int J Rock Mech Min Sci* 48:1045–1054. <https://doi.org/10.1016/j.ijrmms.2011.07.007>
- Fonstad MA, Dietrich JT, Courville BC et al (2013) Topographic structure from motion: a new development in photogrammetric measurement. *Earth Surf Process Landf* 38:421–430. <https://doi.org/10.1002/esp.3366>
- Francioni M, Salvini R, Stead D, Litrico S (2014) A case study integrating remote sensing and distinct element analysis to quarry slope stability assessment in the Monte Altissimo area, Italy. *Eng Geol* 183:290–302. <https://doi.org/10.1016/j.enggeo.2014.09.003>
- Francioni M, Salvini R, Stead D et al (2015) An integrated remote sensing-GIS approach for the analysis of an open pit in the Carrara marble district, Italy: slope stability assessment through kinematic and numerical methods. *Comput Geotech* 67:46–63. <https://doi.org/10.1016/j.compgeo.2015.02.009>
- Gallup D, Frahm JM, Mordohai P, et al (2007) Real-time plane-sweeping stereo with multiple sweeping directions. In: Proceedings of the IEEE Computer Society Conference on computer vision and pattern recognition, p 9
- Ge Y, Tang H, Eldin MAME et al (2015) A description for rock joint roughness based on terrestrial laser scanner and image analysis. *Sci Rep* 5:16999. <https://doi.org/10.1038/srep16999>
- Goessele M, Snaveley N, Curless B, et al (2007) Multi-view stereo for community photo collections. In: Proceedings of the IEEE International Conference on Computer Vision. p 8
- Grasselli G, Egger P (2003) Constitutive law for the shear strength of rock joints based on three-dimensional surface parameters. *Int J Rock Mech Min Sci* 40:25–40. [https://doi.org/10.1016/S1365-1609\(02\)00101-6](https://doi.org/10.1016/S1365-1609(02)00101-6)
- Grasselli G, Wirth J, Egger P (2002) Quantitative three-dimensional description of a rough surface and parameter evolution with shearing. *Int J Rock Mech Min Sci* 39:789–800. [https://doi.org/10.1016/S1365-1609\(02\)00070-9](https://doi.org/10.1016/S1365-1609(02)00070-9)
- Haneberg WC (2008) Using close range terrestrial digital photogrammetry for 3-D rock slope modeling and discontinuity mapping in the United States. *Bull Eng Geol Environ* 67:457–469. <https://doi.org/10.1007/s10064-008-0157-y>
- Haneberg WC, Norrish NI, Findley DP (2006) Digital outcrop characterization for 3-D structural mapping and rock slope design along interstate 90 near Snoqualmie Pass, Washington. In: Proceedings, 57th annual highway geology symposium, Breckenridge, Colorado, p 14
- Heritage GL, Milan DJ (2009) Terrestrial laser scanning of grain roughness in a gravel-bed river. *Geomorphology* 113:4–11. <https://doi.org/10.1016/j.geomorph.2009.03.021>
- ISRM (1978) International society for rock mechanics commission on standardization of laboratory and field tests. In: Suggested methods for the quantitative description of discontinuities in rock masses. *Int J Rock Mech Min Sci*
- Jancosek M, Shekhovtsov A, Pajdla T (2009) Scalable multiview stereo. In: IEEE Workshop on 3D Digital Imaging and Modeling. p 8
- Karekal S, Poropat G, Guo H (2013) Experimental and numerical assessment of shear surface damage using 3D point clouds. *International Symposium on Slope Stability in Open Pit Mining and Civil Engineering*. Perth, Australia, pp 273–280
- Kersten TP (2006) Combination and comparison of digital photogrammetry and terrestrial laser scanning for the generation of virtual models in cultural heritage applications. In: 7th Int. Symp. Virtual Reality, Archaeol. Cult. Herit, p 10
- Khoshelham K, Altundag D, Ngan-Tillard D, Menenti M (2011) Influence of range measurement noise on roughness characterization of rock surfaces using terrestrial laser scanning. *Int J Rock Mech Min Sci* 48:1215–1223. <https://doi.org/10.1016/j.ijrmms.2011.09.007>
- Kim D, Gratchev I, Poropat G (2013a) The determination of joint roughness coefficient using three-dimensional models for slope stability analysis. *International Symposium on Slope Stability in Open Pit Mining and Civil Engineering*. Perth, Australia, pp 281–289
- Kim DH, Gratchev I, Balasubramaniam A (2013b) Determination of joint roughness coefficient (JRC) for slope stability analysis: a case study from the Gold Coast area, Australia. *Landslides* 10:657–664. <https://doi.org/10.1007/s10346-013-0410-8>
- Kim DH, Poropat G, Gratchev I, Balasubramaniam A (2016) Assessment of the accuracy of close distance photogrammetric jrc data. *Rock Mech Rock Eng* 49:4285–4301. <https://doi.org/10.1007/s00603-016-1042-9>
- Kim DH, Balasubramaniam AS, Gratchev I (2018) Application of photogrammetry and image analysis for rock slope investigation. *Geotech Eng J SEAGS AGSSEA* 49:49–56
- Maerz NH, Franklin JA, Bennett CP (1990) Joint roughness measurement using shadow profilometry. *Int J Rock Mech Min Sci* 27:329–343. [https://doi.org/10.1016/0148-9062\(90\)92708-M](https://doi.org/10.1016/0148-9062(90)92708-M)
- Marsch K, Wernecke C (2015) Mapping rock surface roughness with photogrammetry. In: Schubert Kluckner (ed) EUROCK 2015 & Geomechanics Colloquium. Salzburg, Austria, pp 1175–1180
- Mastorocco G, Salvini R, Vanneschi C (2018) Fracture mapping in challenging environment: a 3D virtual reality approach combining terrestrial LiDAR and high definition images. *Bull Eng Geol Environ* 77:691–707. <https://doi.org/10.1007/s10064-017-1030-7>
- Merla G (1951) Geologia dell'Appennino settentrionale. *Boll Della Soc Geol Ital* 70:95–382
- Mills G, Fotopoulos G (2013) On the estimation of geological surface roughness from terrestrial laser scanner point clouds. *Geosphere* 9:1410–1416. <https://doi.org/10.1130/GES00918.1>
- Milne D, Hawkes C, Hamilton C (2009) A new tool for the field characterization of joint. In: Diederichs M, Grasselli G (eds) 3rd CANUS Rock Mechanics Symposium. Canada, Toronto, p 11
- Myers NO (1962) Characterization of surface roughness. *Wear* 5:182–189
- Nilsson M, Vulkan F (2011) Determination of joint shear strength using photogrammetry. Luleå University of Technology, Luleå, Sweden
- Nocchi M (1960) Osservazioni sulla stratigrafia e cenni sulla tettonica della parte meridionale dei Monti del Chianti. *Boll Della Soc Geol Ital* 79:217–356

- Pandeli E, Fazzuoli M, Sandrelli F et al (2018) The scaglia toscana formation of the monti del chianti: new lithostratigraphic and biostratigraphic data. *Ital J Geosci* 137:38–61. <https://doi.org/10.3301/IJG.2017.16>
- Patton FD (1966) Multiple modes of shear failure in rock and related materials. University of Illinois, Urbana–Champaign, USA
- Poropat G (2008) Remote characterization of surface roughness of rock discontinuities. In: Potvin Y, Carte J, Dyskin A, Jeffrey R (eds) International Rock Mechanics Symposium, Perth, pp 447–458
- Poropat G V (2009) Measurement of surface roughness of rock discontinuities. In: ROCKENG09: Proceedings of the 3rd CANUS Rock Mechanics Symposium, p 9
- Riquelme A, Cano M, Tomás R, Abellán A (2017) Identification of rock slope discontinuity sets from laser scanner and photogrammetric point clouds: a comparative analysis. *Proc Eng* 191:838–845. <https://doi.org/10.1016/j.proeng.2017.05.251>
- Salvini R, Francioni M, Riccucci S et al (2011) Stability analysis of “Grotta delle Felci” Cliff (Capri Island, Italy): structural, engineering-geological, photogrammetric surveys and laser scanning. *Bull Eng Geol Environ* 70:549–557
- Salvini R, Mastrorocco G, Seddaiu M et al (2017) The use of an unmanned aerial vehicle for fracture mapping within a marble quarry (Carrara, Italy): photogrammetry and discrete fracture network modeling. *Geomat Nat Hazards Risk* 8:34–52. <https://doi.org/10.1080/19475705.2016.1199053>
- Salvini R, Mastrorocco G, Esposito G et al (2018) Use of a remotely piloted aircraft system for hazard assessment in a rocky mining area (Lucca, Italy). *Nat Hazards Earth Syst Sci* 18:287–302. <https://doi.org/10.5194/nhess-18-287-2018>
- Schmidt A, Schilling A, Maas H-G (2012) A method for the registration of hemispherical photographs and TLS intensity images. In: ISPRS—International Archives of the photogrammetry, remote sensing and spatial information sciences, p 5
- Schneider D, Schwalbe E (2008) Integrated processing of terrestrial laser scanner data and Fisheye-camera image data. In: International Archives of photogrammetry, remote sensing and spatial information science. p 6
- Schwalbe E, Maas HG, Kenter M, Wagner S (2009) Hemispheric image modeling and analysis techniques for solar radiation determination in forest ecosystems. *Photogramm Eng Remote Sens* 4:375–384. <https://doi.org/10.14358/PERS.75.4.375>
- Sirkkiä J, Kallio P, Iakovlev D, Uotinen L (2016) Photogrammetric calculation of JRC for rock slope support design. In: Nordlund E, Jones T, Eitzenberger A (eds) Proceedings of the 8th International Symposium on ground support in mining and underground construction, pp 622–634
- Rahman Z, Slob S, Hack R (2006) Deriving roughness characteristics of rock mass discontinuities from terrestrial laser scan data. In: IAEG 2006, Geological Society of London, London, UK, paper 437
- Spetsakis M, Aloimonos JY (1991) A multi-frame approach to visual motion perception. *Int J Comput Vis* 6:245–255. <https://doi.org/10.1007/BF00115698>
- Sturzenegger M, Stead D (2009) Close-range terrestrial digital photogrammetry and terrestrial laser scanning for discontinuity characterization on rock cuts. *Eng Geol* 106:163–182. <https://doi.org/10.1016/j.enggeo.2009.03.004>
- Sturzenegger M, Yan M, Stead D, Elmo D (2007) Application and limitations of ground-based laser scanning in rock slope characterization. In: Eberhardt E, Stead D, Morrison T (eds) Proceedings 1st Canada–U.S. Rock Mechanics Symposium. Vancouver, pp 29–36
- Tatone BSA, Grasselli G (2009) A method to evaluate the three-dimensional roughness of fracture surfaces in brittle geomaterials. *Rev Sci Instrum* 80:125110. <https://doi.org/10.1063/1.3266964>
- Tse R, Cruden DM (1979) Estimating joint roughness coefficients. *Int J Rock Mech Min Sci Geomech Abstr* 16:303–307. [https://doi.org/10.1016/0148-9062\(79\)90241-9](https://doi.org/10.1016/0148-9062(79)90241-9)
- Unal M, Yakar M, Yildiz F (2017) Discontinuity surface roughness measurement techniques and the evaluation of digital photogrammetric method. In: Commission III, WG III/2, p 6
- Valduga A (1948) Osservazioni geologiche sulla parte settentrionale dei Monti del Chianti. *Boll Della Soc Geol Ital* 67:161–187
- Valduga A (1952) Cenni sulla stratigrafia e osservazioni sulla tettonica della parte centrale dei Monti del Chianti. *Boll Della Soc Geol Ital* 71:3–41
- Vanneschi C, Salvini R, Massa G et al (2014) Geological 3D modeling for excavation activity in an underground marble quarry in the Apuan Alps (Italy). *Comput Geosci* 69:41–54. <https://doi.org/10.1016/j.cageo.2014.04.009>
- Vanneschi C, Eyre M, Francioni M, Coggan J (2017) The use of remote sensing techniques for monitoring and characterization of slope instability. *Proc Eng* 191:150–157. <https://doi.org/10.1016/j.proeng.2017.05.166>
- Westoby MJ, Brasington J, Glasser NF et al (2012) “Structure-from-Motion” photogrammetry: a low-cost, effective tool for geoscience applications. *Geomorphology* 179:300–314. <https://doi.org/10.1016/j.geomorph.2012.08.021>

Publisher’s Note Springer Nature remains neutral with regard to jurisdictional claims in published maps and institutional affiliations.